Modelling *Anopheles gambiae* Mosquito Population Dynamics in Heterogeneous Landscapes

Laura Anne Bissett

MSc, BSc

Submitted in fulfilment of the requirements for the

Degree of Master of Science by Research

School of Biodiversity, One Health, and Veterinary Medicine

College of Medical, Veterinary, and Life Sciences

University of Glasgow

February 2026

Abstract

The aim of this project is to develop a generalisable mathematical framework to model the population dynamics of *Anopheles gambiae* mosquitoes in a heterogeneous landscape. The model incorporates environmental dependencies (temperature and rainfall), with mosquito life history traits (development, survival, and gonotrophic cycle). Two approaches to model temporary habitat are tested in conjunction with the population dynamics framework, which regulate the environmental carrying capacity of the larvae population. The model is then validated against adult mosquito abundance data that was collected from villages in Burkina Faso and Nigeria. The evaluation of these temporary habitat models demonstrate the key mechanisms that drive the changes in mosquito population dynamics. The model is then used to predict a mosquito population in Burkina Faso (in the absence of control), where it is shown that without the implementation of the intervention, the mosquito population would be significantly higher than the observed abundance.

Contents

Acknowledgements **8**

Author's Declaration **9**

1 Introduction **10**

1.1 *Anopheles* Mosquitoes and Malaria 10

1.2 Environmental Influence on Mosquito Population Dynamics 12

1.3 Modelling *Anopheles* Population Dynamics 15

1.4 Research Objectives 18

1.5 Summary 18

2 Materials and Methods **20**

2.1 Population Dynamics Model Framework 20

2.2 Model Parameterisation 22

2.2.1 *Anopheles* Mosquito Life History Traits 22

2.2.2 Habitat Availability (w_{temp}) 30

2.3 Numerical Simulations 33

2.4 Validation of Population Dynamics Model 34

2.4.1 Burkina Faso 34

2.4.2 Nigeria 35

2.5 Field Surveillance Data from Burkina Faso 35

3 Results **36**

3.1 Evaluating the Changes in Shape and Size of Temporary Habitat Models . . 36

3.1.1 Tompkins Model 36

3.1.2 Eikenberry Model 37

3.2 Population Dynamics Model Validation 38

3.2.1 Tengrela, Burkina Faso 38

3.2.2 Garki District, Nigeria 42

3.3 Population Dynamics of *Anopheles gambiae* in Burkina Faso 47

4 Discussion **50**

List of Tables

1 Table of parameter values used in model 33

2 Values of R^2 for Tompkins and Eikenberry model in Tengrela, Burkina Faso. 40

3 Values of R^2 for Tompkins and Eikenberry model in Garki District, Nigeria. 45

List of Figures

1 Map of distribution of *Anopheles gambiae s.l.* in Africa, taken from Lanzaro et al. [1]. 11

2 Life-cycle of *Anopheles gambiae* mosquito. Adult mosquitoes lay their eggs in stagnant water, after a period of a few days they develop into larvae. During the larval stage those that survive will pupate, and thereafter emerge as adults. 12

3 Schematic of the life cycle model framework. Adults (A) lay eggs (E) at a rate $b(t)$, which either mature $M_E(t)$ or die at a rate $\delta_E(T(t))$. After, maturation eggs are recruited into the larvae (L) stage $R_L(t)$ where they either mature into pupae $M_L(t)$, die at a rate $\delta_L(T(t))$ or die due to density-dependence $\delta_{DD}(t)$. After maturation they are recruited into the pupae (P) stage $R_P(t)$ where they either mature $M_P(t)$ or die at a rate $\delta_P(T(t))$, from which they are then recruited into the adult stage $R_A(t)$ and lay eggs again or die at a rate $\delta_A(T(t))$. Classes that are coloured blue represent the aquatic stages. 21

4 Thermal performance of the gonotrophic cycle. Each point represents the duration of the gonotrophic cycle at a specific temperature, and the points are coloured corresponding to which study the data came from [2–6]. The shape of the points represents the corresponding species. A Brière function was fitted to the dataset giving $R^2 = 0.844$ 24

5 Thermal performance of egg development and through-stage survival over a temperature range $10-40^{\circ}C$. **A:** Gaussian function fit to *Anopheles gambiae* development data from [7] with $R^2 = 0.823$ **B:** Gaussian function fit to *Anopheles arabiensis* data from [8] with $R^2 = 0.929$. 25

6 Thermal performance of larvae development and through-stage survival at a temperature range of $10-40^{\circ}C$. **A:** Gaussian function fit to *Anopheles gambiae* development data from [7,9] with $R^2 = 0.865$ **B:** Gaussian function fit to data from [2,7,10] with $R^2 = 0.869$. 27

7 Thermal performance of pupae development and through-stage survival at temperature range $10-40^{\circ}C$. **A:** Gaussian function fit to *Anopheles gambiae* development data from [7] with $R^2 = 0.806$, **B:** Gaussian function fit to data from [7] with $R^2 = 0.935$. 29

8 Thermal performance of adult longevity at temperature range $10-40°C$, and humidity levels $40-100\%$. Data for *Anopheles gambiae* taken from [7] was used for the fitting, with a Gaussian function fit to data at each humidity level. Each coloured point and line represent the observed data and corresponding reaction norm, respectively, at each level of humidity. 30

9 Schematic of the processes involved in the formation of a viable habitat. Water fills a ground depression by precipitation falling directly onto the surface area $A(t)$, or falling on the area inside the depression yet to be covered by water which a fraction of then contributes to the filling of the site R_{frac}. Water is lost through evaporation $E_v(T(t))$ and infiltration into the soil I. The maximum the site can reach is w_{max}. Blue arrows correspond to the water gain/loss in the site. 31

10 Fractional habitat coverage under continuous rainfall conditions of Tompkins model [11] **A:** when R_{frac} is varying with each coloured line representing a different condition, and **B:** when λ varies from $1/100-1/1000$ where each coloured line represents a different value. Where no rainfall occurred between day 500-750, otherwise rainfall $R(t) = 100$ mm to represent the dry and wet season, respectively and parameters as shown in Table 1. 36

11 Fractional habitat coverage under continuous rainfall conditions of Eikenberry model [12] **A:** when R_{frac} is varying with each coloured line representing a different condition, **B:** when p is varied from $1-2$ where each coloured line represents a different value, and **C:** when h_{max} is varied from $12-100$. Where no rainfall occurred between day 500-750, otherwise rainfall $R(t) = 100$ mm to represent the dry and wet season, respectively and parameters as shown in Table 1. 37

12 Environmental Conditions, Tengrela. Each panel shows environmental data from 2018-2023 for **A:** Temperature, **B:** Habitat coverage generated by Eikenberry model where each coloured line represents a different run-off model, **C:** Habitat coverage generated by the Tompkins model where each coloured line represents a different combination of λ and R_{frac}. 39

13 Population dynamics of female mosquito population in Tengrela, Burkina Faso, from 2018-2023 using the Tompkins habitat model. Each coloured line represents a different combination of λ and R_{frac}, and transparent blue panels depict the wet season. **A:** normalised larvae abundance per km^2, **B:** larvae survival, **C:** normalised female adult mosquito abundance where coloured lines are the model prediction and black points are unpublished observed data. 40

14 Population dynamics of female mosquito population in Tengrela Burkina Faso over time series 2018-2023 using the Eikenberry model for habitat. Each coloured line represents a different combination of R_{frac}, and transparent blue panels depict the wet season. **A:** normalised larvae abundance per km^2, **B:** larvae survival, **C:** normalised female adult mosquito abundance where coloured lines are the model prediction and black points are unpublished observed data. 41

15 1-1 ratio plot of model prediction vs observed data in Tengrela, Burkina Faso, from 2018-2023 using the Tompkins habitat model. Points are coloured by season either dry (green) or wet (purple) for each combination of λ and R_{frac}; **A:** $\lambda = 1/1000, R_{frac} = 1$, **B:** $\lambda = 1/1000, R_{frac} = 0.5$, **C:** $\lambda = 1/500, R_{frac} = 1$, and **D:** $\lambda = 1/500, R_{frac} = 0.5$ 42

16 1-1 ratio plot of model prediction vs observed data in Tengrela Burkina Faso over time series 2018-2023 using the Eikenberry model for habitat. Points are coloured by season either dry (green) or wet (purple) for each combination R_{frac}; **A:** $R_{frac} = 1 - \frac{w}{wmax}$, **B:** $R_{frac} = 1$, **C:** $R_{frac} = 0.5$, and **D:** $R_{frac} = 0.01$ 42

17 Garki District environmental data from 1971-1973. **A:** Temperature, **B:** Habitat coverage generated by Eikenberry model where each coloured line represents a different run-off model, **C:** Habitat coverage generated by the Tompkins model where each coloured line represents a different combination of λ and R_{frac}. 43

18 Population dynamics of female mosquito population in Garki District Nigeria (Village 3), from 1971-1973, using the Tompkins habitat model. Each coloured line represents a different combination of λ and R_{frac}, and transparent blue panels depict the wet season. **A:** larvae abundance per km^2, **B:** larvae survival, **C:** female adult mosquito abundance where coloured lines are the model prediction and black points are unpublished observed data. . . 44

19 Population dynamics of female mosquito population in Garki District Nigeria over time series 1971-1973 using the Eikenberry model for habitat. Each coloured line represents a different combination of λ and R_{frac}, and transparent blue panels depict the wet season. **A:** larvae abundance per km^2, **B:** larvae survival, **C:** female adult mosquito abundance where coloured lines are the model prediction and black points are unpublished observed data. . . 45

20 1-1 ratio plot of model prediction vs observed data in Garki District Nigeria (Village 3), from 1971-1973, using the Tompkins habitat model. Points are coloured by season either dry (green) or wet (purple) for each combination of λ and R_{frac}; **A:** $\lambda = 1/1000, R_{frac} = 1$, **B:** $\lambda = 1/1000, R_{frac} = 0.5$, **C:** $\lambda = 1/500, R_{frac} = 1$, and **D:** $\lambda = 1/500, R_{frac} = 0.5$ 46

21 1-1 ratio plot of model prediction vs observed data in Garki District Nigeria over time series 1971-1973 using the Eikenberry model for habitat. Points are coloured by season either dry (green) or wet (purple) for each combination R_{frac}; **A:** $R_{frac} = 1 - \frac{w}{wmax}$, **B:** $R_{frac} = 1$, **C:** $R_{frac} = 0.5$, and **D:** $R_{frac} = 0.01$ 46

22 Predicted female mosquito adult abundance in village clusters 21-25 in the AvecNet Trial [13]. The black line is the predicted abundance from the DDE model using the Tompkins temporary habitat model [11], with $\lambda = 1/500$ and $R_{frac} = 0.5$. Each red point is the observed adult abundance in a month, and the green dashed line is when the intervention was introduced. The transparent blue panels highlight the duration of the wet season. 47

23 Life-history traits of *Anopheles gambiae* mosquitoes. Transparent blue panels indicate the wet season. Each panel depicts a life history trait **A:** development rate, **B:** through-stage survival, and **C:** duration of the gonotrophic cycle. 48

24 Life-history traits of *Anopheles gambiae* mosquitoes. Transparent blue panels indicate the wet season. Each panel depicts a life history trait **A:** Egg development rate, **B:** Egg through-stage survival, **C:** Pupae development rate, and **D:** Pupae through-stage survival. 49

Acknowledgements

I would like to thank my supervisors Doctor Mafalda Viana, Professor Christina Cobbold, and Professor Heather Ferguson for their support and guidance throughout my research project. I would also like to thank Professor Pablo Murcia for always being there to offer his advice whenever I've needed it. Finally, thank you to my family for always supporting me in everything that I do, I am beyond grateful.

Author's Declaration

I declare that, except where explicit reference is made to the contribution of others, that this thesis is the result of my own work and has not been submitted for any other degree at the University of Glasgow or any other institution.

LAURA ANNE BISSETT

1 Introduction

1.1 *Anopheles* Mosquitoes and Malaria

Vector-borne diseases (VBD) are diseases transmitted to humans primarily through the bite of infected arthropods, such as mosquitoes and ticks, and have devastating consequences worldwide. Over half a million deaths globally each year and more than 17% of all infectious disease cases can be attributed to a VBD [14]. Mosquito-borne pathogens such as dengue fever and malaria cause some of the largest outbreaks in tropical regions [14].

Of all VBDs that can infect humans, malaria is the largest burden on public health. Malaria is a VBD pathogen caused by the distribution of plasmodium parasites through the bite of an infected female *Anopheles* mosquito [15]. Transmission is exclusively through human and mosquito contact, and cannot be contracted via human to human interaction. Once a mosquito becomes infected the parasite is incubated for a period of 7-18 days depending on the parasite species [16], after which they will stay infectious for the rest of their lifetime.

Malaria is one of the greatest public health concerns globally, primarily occurring in tropical and subtropical regions, and is now endemic in 80 countries [14, 17]. From the year 2000, malaria cases and deaths were consistently declining until 2015, however over the last few years this progress has plateaued with annual cases increasing by nine million from 2023 to 2024 and deaths increasing by 12,000 [17]. The burden of disease in Africa is most extensive, with the World Health Organisation reporting that this region alone accounts for approximately 95% of cases and deaths recorded, with most deaths occurring in children under the age of five [17].

There are several different species of *Anopheline* mosquitoes that transmit malaria, each with their own unique population dynamics and vectorial capacities. Throughout Africa, the primary vectors for malaria transmission are the *Anopheles gambiae* complex and *Anopheles funestus* [15, 18–20](Figure 1). Broadly, the life cycle of these vectors and other mosquitoes consists of four main stages egg, larva, pupa, and adult (Figure 2). Adult female mosquitoes lay their eggs in stagnant pools of water; however the size of breeding habitats can range from large irrigated farming areas to small pools and puddles created by precipitation, based on species preference as well as site availability [15, 21, 22]. Eggs then undergo a period of

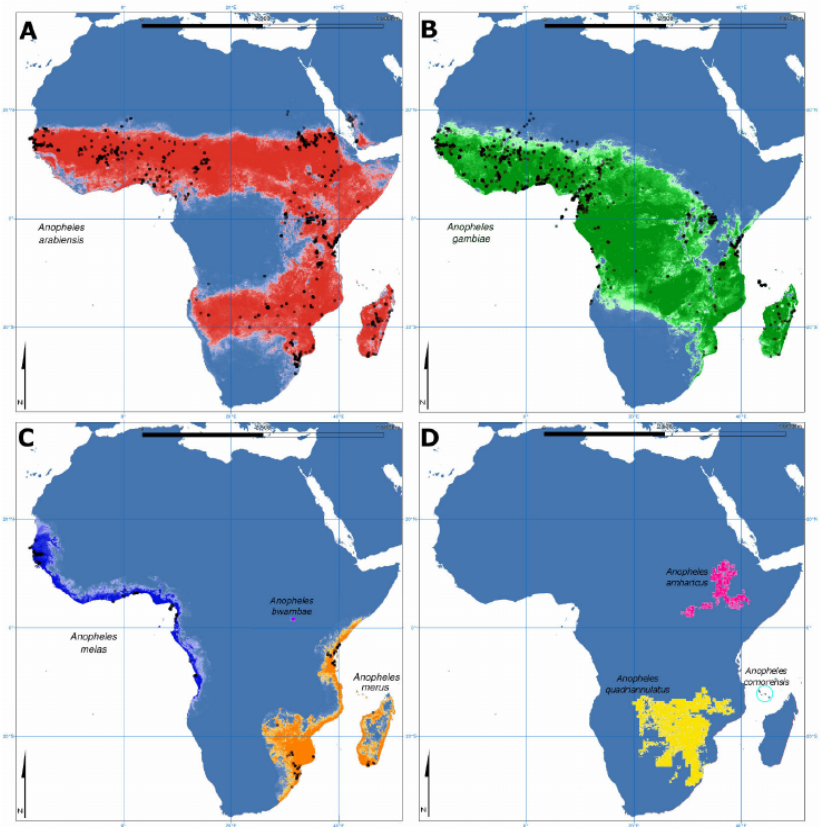

Figure 1: Map of distribution of *Anopheles gambiae s.l.* in Africa, taken from Lanzaro et al. [1].

development which is typically around one day before maturing into larvae depending on environmental temperature [22, 23]. Several factors influence the rate (development time) and success (survival to emergence) of larval development of African malaria vectors; including changes in the surrounding environment (a more detailed description given in Section 1.2) [2, 7, 22, 24, 25], and density-dependent mortality [5, 6, 26–28] due to overcrowding. Larvae that survive this stage mature to become pupae, undergo further development before emerging as adults. In order for female adults to develop and lay their eggs, they not only have to find a mate but also find a suitable blood meal; during which transmission can occur. This process from feeding to laying eggs is called the gonotrophic cycle. After females lay their eggs, they then become host-seeking again, and the cycle repeats [22]. The longevity of an adult mosquito strongly depends on ambient temperature [2, 4, 7, 9, 29–31], and they are most commonly found in tropical and subtropical environments showing a preference for warmer climates [1, 22, 23].

In the majority of malaria endemic areas several mosquito species cohabit, each with their own behaviour characteristics. This makes it challenging when deploying intervention strategies. *Anopheles gambiae s.s.* mosquitoes typically feed and rest indoors [15, 22], however species such as *Anopheles arabiensis* feed outdoors [15, 22]. Currently, efforts to reduce

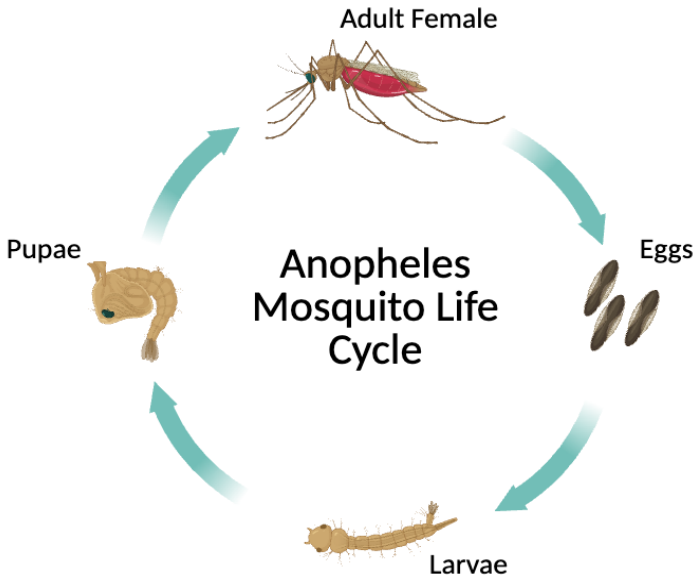

Figure 2: Life-cycle of *Anopheles gambiae* mosquito. Adult mosquitoes lay their eggs in stagnant water, after a period of a few days they develop into larvae. During the larval stage those that survive will pupate, and thereafter emerge as adults.

malaria transmission in endemic regions are primarily focussed on controlling vector populations. Intervention methods such as insecticide treated bed nets (ITNs) and indoor residual spraying (IRS) have been the most commonly distributed approaches [15, 32, 33]. These approaches exploit the natural feeding behaviour of Anopheline species, which primarily - but not exclusively - involves feeding and resting indoors, with biting often taking place during the night when people would be protected by a bed net. However, as preventative measures have been more widely adopted as the burden of malaria increases, pyrethroid resistance in *Anopheles* mosquitoes has also rapidly increased [34, 35]. Although, new insecticides are being developed, [36] the innate issue remains the same in that the mosquitoes have the ability to adapt their behaviours and genetic make-up to develop resistance [37]. Therefore, in areas where there are two species with different biting behaviours cohabiting, the use of only indoor based strategies such as ITNs and IRS – even if combined – is not necessarily an effective approach [32, 34]. Given that different species have different vectorial capacities, this could have important implications for how malaria is managed, however the impact interventions have on the broader community composition is not known.

1.2 Environmental Influence on Mosquito Population Dynamics

Anopheles mosquitoes are an ectothermic species, which means their body temperature is regulated by their surrounding environment, and changes in ambient temperatures can influence their ecology and behaviour characteristics to varying degrees [4, 29, 31, 38, 39].

Life-history traits such as the time taken for a mosquito to metamorphose from egg to adult, survival at each life stage, and the length of time taken for a female adult to lay their eggs are all dictated by the temperature mosquitoes experience [22, 23, 29]. For example, in a study carried out by Bayoh [7], they investigated the temperature impacts on *Anopheles gambiae* mosquito development and survival during all aquatic life stages across a wide range of temperatures ($10-40°C$). They found that mosquitoes did not survive the larvae stage when temperatures dropped below $18°C$ or exceeded $32°C$. This is in contrast with a later study by Kirby et al. [10], who found that *Anopheles gambiae* larvae survived up to temperatures of $35°C$, albeit at very low levels ($< 10\%$). Both studies however, found the same optimal temperature for survival at $25°C$ [7, 10]. Bayoh [7] also examined larval development across the same temperature range ($10-40°C$), finding an optimum temperature of $28°C$. No development however could be reported at temperatures $< 18°$ as the larvae did not survive. Survival of *Anopheles gambiae* was also investigated in a later study by Barreaux et al. [9], however their experiment was only conducted at three temperature values ($21, 25, 29°C$). Despite this study not investigating a wide range of temperature values, the results were in line with those of Bayoh [7], finding a thermal optimum for development of $29°C$.

Temperature variation has a profound impact on the longevity of adult Anopheline mosquitoes. Christiansen-Jucht et al. [29] showed that changes in temperature can prolong the life span of *Anopheles gambiae* mosquitoes. They found that at $27°C$ adults can survive as long as 31 days, however when temperatures increased by $4°C$, this survival was reduced by six days [29]. A later study by Barreaux et al. [9], found similar results where adult longevity decreased by eight days when temperatures declined from $29°C$ to $25°C$ (surviving 21 and 29 days, respectively).

The gonotrophic cycle is also influenced by temperature, and increases in temperatures by just one or two degrees can reduce the duration of the gonotrophic cycle [4–6]. Armstrong et al. [4] conducted experiments on the duration of the gonotrophic cycle of *Anopheles gambiae* mosquitoes at four temperatures ($21, 24, 27, 30°C$). They found that at $21°C$ the duration of the cycle was six days; however this reduced to four days at the remaining temperatures. In line with these results, a later study by Christiansen-Jucht et al. [3] measured the duration of the gonotrophic cycle of *Anopheles gambiae* at three temperature values ($23, 27, 31°C$) across three cycles. They found that for all temperatures, during the first gonotrophic cycle, the duration was approximately four days. Agyekum et al. [2] also tested the gonotrophic

cycle duration at three temperatures ($25, 28, 30^{\circ}C$), however they found that the duration was lower, approximately three days across all temperatures.

These temperature dependencies are extremely important as if mosquitoes are developing more quickly and surviving for longer in malaria endemic regions, this can result in an increase in the population and therefore an increase in the risk of malaria transmission [23]. These studies also demonstrate that the relationships between temperature and mosquito life history are non-linear, with temperatures increasing to an optimum value and then declining. These non-linear relationships are important to consider when developing a model, and steer us away from setting temperature at a fixed constant.

Sustaining mosquito populations is not only linked with temperature but also with precipitation. As mentioned, *Anopheles gambiae* mosquitoes in particular have a preference for laying their eggs in small temporary aquatic habitats such as puddles and ditches which are generally formed by rainfall [15, 21, 23]. In order for these pools to be viable habitats they must exist long enough for the aquatic stage of metamorphosis to be completed and for the mosquitoes to become adults [40]. Aquatic habitats also require an initial period of rainfall in order for them to form, thought to be around 10-14 days [7, 29]. These habitats are important as they regulate the early stages of the mosquito life cycle. If there are not enough instances of permanently viable habitats in the surrounding environment, temporary habitats (e.g. puddles) can become overcrowded. This can result in induced mortality through competition for space and/or food [41]. At the larval stage, this density-dependent mortality can have large effects on the survival of larvae [5, 6, 26–28] in particular, as mosquitoes spend the majority of the aquatic stage in this phase of the life cycle [7]. Other factors such as washout can occur. This phenomenon can happen during periods of intense rainfall, where these temporary habitats can reach their capacity and overflow, resulting in a loss in the population [42]. More generally, the association between vector populations and rainfall is positive, such that as rainfall increases the growth of temporary habitats also increase, creating more viable habitat [43, 44] .

As *Anopheles* mosquito populations exhibit strong seasonal dynamics, it is important to consider how the population is sustained, given that during the dry season temporary habitats are scarce due to a lack of sufficient rainfall [45]. Species such as *Anopheles funestus* are also found in permanent habitats (e.g. larger ponds, streams or irrigated habitats) that are stable

year round, therefore the utilisation of these habitats could be a method for sustaining populations at low levels throughout the dry season [21, 41]. In some species such as *Anopheles colluzzi*, there is evidence of aestivation [45]. This means that over the dry season, the population can become dormant and then the start of the rainy season they exit this dormancy and it triggers a reemergence in the population. However, for *Anopheles gambiae* there has been a lack of evidence that this occurs in this species. *Anopheles* mosquitoes are one of the few mosquitoes that travel long distances, and therefore it is thought that a potential method of sustaining populations is migration [45]. This idea suggests that at the beginning of the dry season mosquito populations will disperse to an area where there is enough viable habitat to sustain the population and then they return during the wet season. However, this is extremely difficult to quantify as it involves being able to track specific mosquitoes. Genetic analysis of the population could be employed to infer dispersal patterns across the landscape, however with a lack of knowledge of where they may travel to it is difficult to accurately measure in the field.

1.3 Modelling *Anopheles* Population Dynamics

Modelling has been instrumental in understanding the population dynamics of *Anopheles* mosquitoes. Traditionally, systems of ordinary differential equations (ODEs) have been adopted to explore population dynamics [11,12,46–48], mainly due to their ability to capture complex biological mechanisms whilst remaining computationally efficient. For example, White et al. [46] developed a model using continuous differential equations to investigate the population dynamics of *Anopheles* mosquitoes, which incorporated temperature dependencies for some traits such as development and mortality, as well as considering rainfall dependencies to regulate larval populations through density-dependent survival. The model incorporated several processes that have proved to be important in understanding mosquito populations, but its simplicity meant that some less well known relationships such as between temperature and gonotrophic cycle, were assumed constant at their experimental optimum [46], and the rainfall-dependent carrying capacity was integrated as the amount of cumulative rainfall over time [46]. The latter meant the model was very region-specific as it involved a user-defined tuning parameter for the dataset, which resulted in some restrictions in the subsequent applications of the model [46]. The abundance data they used was also historical, from a project carried approximately 50 years ago, and therefore due to extreme environmental changes the results may not be as informative for the today's landscape. Mordecai et al. [48] also adopted a system of ODEs to explore the impact of temperature on

malaria transmission, and utilised thermal response curves to investigate temperature effects on mosquito and parasite life histories. They supported their findings using published data relating to the risk of malaria in Africa, but due to a lack of data availability on *Anopheles* mosquitoes in temperature controlled environments, their model was informed from multiple mosquito species [48]. For example, they inferred their fecundity parameter from an entirely different mosquito species (*Aedes albopictus*) which has very different breeding characteristic to *Anopheles* mosquitoes [48]. Parham and Michael [49] used mathematical models to investigate the effects of temperature and rainfall on malaria transmission. They also considered the impact these environmental factors could have on mosquito population dynamics. It was concluded that rainfall had a great impact on the ability to achieve malaria extinction as it influenced the emergence of mosquito vectors [49].

There has been an extensive body of work carried out evaluating the effect of environmental variation on malaria vector population dynamics [46, 48–53]. Most models focus primarily on the influence of temperature, as this has been shown to have the greatest impact on life history traits such as development, survival, and the gonotrophic cycle. The influence of precipitation has been less studied, and in particular the influence on temporary habitats (which are dependent on rainfall levels). Particularly for mosquito species such as *Anopheles gambiae*, the creation and loss of breeding sites greatly influences the population dynamics as they are reliant on these habitats to lay their eggs [40, 54, 55]. Rainfall-dependent density-dependence at larval survival stages is often included in population dynamics models [56], but the relationship is generally assumed to be linear or quadratic which makes it difficult to dissect the mechanisms linked to breeding habitats that are driving the changes in the density-dependence of larvae.

Tompkins et al. [11] developed a simple water balance model to allow for this consideration. They developed an ODE model that incorporated the processes that contribute to the creation and sustainment of temporary habitats. This model calculated the fraction of temporary habitat available at each time-step, and then in combination with the amount of larvae that fraction could sustain gave an environmental carrying capacity. There were several simplifying assumptions made, such as the relationship between the amount of precipitation and the growth of potential habitats which they assume to be linear. A later study carried out by Asare et al. [54], extended this framework to provide a better description between water volume and habitat growth. This model considered the geometry of a viable habitat

using reference pools, and also allowed for the incorporation of run-off from the surrounding environment. This provided a more realistic approach to the mechanisms involved in the formation of temporary habitats. These models were then used in conjunction with systems of ODEs to describe the population dynamics of *Anopheles* mosquitoes.

More complex frameworks such as the use of delay-differential equations have also been utilised to overcome the shortcomings, as described above, of ODE models [52, 53, 57]. For example, Nisbet and Gurney [58] developed a framework that incorporated delays into models, which means that population in each stage is directly influenced by the life history in the previous stages. This framework allows the incorporation of the effect of smaller temperature fluctuations through each life-stage compared with instantaneous transitions that are unable to be accounted for when using ODE models, as in DDE models environmental variation is carried through the life stages. As temperature has a major effect on parameters such as development and survival, it is more realistic to assume that individuals would experience varying temperatures during the life stages. This framework has proven to be advantageous when investigating other mosquito genus such as *Culex pipiens* and *Aedes albopictus* [57,59], however, has not been widely used for investigating *Anopheles* mosquito population dynamics. One of the first implementations of this framework for *Anopheles* mosquitoes was by Beck-Johnson et al. [52]. This study had a stage-structured model that was used to explore the temperature effects on *Anopheles* mosquitoes. The model was parameterised using thermal performance curves, however data from multiple different mosquito species for various traits was used. For example, they utilised data from *Anopheles stephensi* to describe the effects of density-dependence, and *Anopheles gambiae* for development and survival. These mosquito species have different behavioural characteristics, in particular *Anopheles stephensi* tend to utilise small permanent sites such as containers and are often found in urban areas [60], compared with *Anopheles gambiae* which prefer temporary breeding habitats and found in more rural areas [61]. Although this study accounts for all life stages of *Anopheles* mosquitoes, they utilise development data that tracks the total duration from egg to adult emergence, rather than the time taken to progress to each stage individually, and then assume a constant proportion of the egg, larvae, and pupae are in each class at every time-step. This is a simplifying assumption and may cause discrepancies in the predicted population dynamics, as in reality this would unlikely be a constant proportion based on variation in environment parameters.

This premise of this study is to develop a mathematical framework that can evaluate the population dynamics of *Anopheles gambiae* mosquitoes, whilst also accounting for the major factors that are known to influence the system. The model consists of a system of stage-structured delay differential equations, parameterised by thermal performance curves that have been fitted to a wide range of data from the literature with a focus on *Anopheles gambiae*. Mosquito life-history traits are temperature-dependent; however the model also accounts for rainfall-dependencies in the form of an environmental carrying capacity which is developed using a habitat model for temporary breeding sites. I hypothesise that incorporating these additional complexities in model formulation will enable more accurate prediction of real world dynamics. This can be assessed by comparing the fit of deterministic models parameterised by relevant data, to independent field surveillance.

1.4 Research Objectives

The main objective of this project is to develop a generalisable delay-differential equation (DDE) framework for the population dynamics of *Anopheles gambiae* mosquitoes. The model will be parameterised by thermal performance curves for specific life-history traits and incorporate a model for temporary habitats in the larvae stage. More specifically, the aim is to

1. Identify key mechanisms for modelling temporary habitat availability

2. Validate the developed modelling framework against long-term field surveillance data

3. Describe mosquito population dynamics for a village in the Cascades region of Burkina Faso, in the absence of control measures

1.5 Summary

The main focus of this thesis is to develop a general framework to model *Anopheles gambiae* mosquito population dynamics. This thesis will begin by introducing a system of DDEs that model each stage of the *Anopheles gambiae* life cycle. The model is then parameterised by thermal performance curves for mosquito traits such as egg, larvae and pupae development and survival, the gonotrophic cycle, as well as female adult survival. Two habitat models are introduced, one more complex than the other. Both models explore the formation of

temporary pools and are implemented into the main model framework by means of the carrying capacity term, which accounts for both temporary and permanent breeding habitats. These models are then used to explore the best way to model temporary breeding habitats, first under constant rainfall conditions which allows the exploration of the effect the terms in the model have on the dynamics and secondly under varying rainfall. After, the models are utilised in conjunction with the stage-structured population dynamics model and validated against long-term adult abundance data for *Anopheles gambiae* mosquitoes in Burkina Faso and Nigeria. The long term surveillance data from Burkina Faso is from Tengrela, and the data from Nigeria was collected as part of the Garki Project [62]. The models will be evaluated across the entire time series which allows the exploration of between season dynamics as well as single season nuances between the observed and predicted data. Finally, the model will be used to predict a population of mosquitoes in a village in Burkina Faso (independent of the data used for validation) in the absence of control measures.

2 Materials and Methods

2.1 Population Dynamics Model Framework

The model is based on the framework first presented by Nisbet and Gurney (1983) [58], and consists of delay-differential equations (DDEs) that represent the main life stages of female *Anopheles* mosquitoes: egg (E), larvae (L), pupae (P), and adults (A), at time (t) per km^2. The key characteristics of the model are that each of the life history stages are environmnent-dependent through thermal performance curves, as well as some of the rates between them, in particular larvae survival, which has density-dependent mortality influenced by larvae habitat features. The model also accounts for the impact of environmental dependence, as well as density-dependent mortality. Here, due to lack of data availability, although it is known that during the larvae stage of the life cycle there are four different instars, it is assumed that this is a single larvae class. A schematic of the model is shown in Figure 3:

$$\frac{dE(t)}{dt} = R_E(t) - M_E(t) - \delta_E(T(t))E(t), \tag{1}$$

$$\frac{dL(t)}{dt} = R_L(t) - M_L(t) - \Big(\delta_L(T(t)) + \delta_{DD}(t)L(t)\Big)L(t), \tag{2}$$

$$\frac{dP(t)}{dt} = R_P(t) - M_P(t) - \delta_P(T(t))P(t), \tag{3}$$

$$\frac{dA(t)}{dt} = R_A(t) - \delta_A(T(t))A(t). \tag{4}$$

The recruitment $R_i(t)$ into a life stage and maturation $M_i(t)$ out of a life stage are the transition from one class to the next, and $\delta_i(T(t))$ denotes the temperature-dependent (T) mortality rate (where $i = E, L, P, A$). During the larval stage of the mosquito life-cycle, mortality can also occur due to density-dependence denoted by $\delta_{DD}(t)$ which is a result of competition for space and food within habitats at time t [26, 27]. The recruitment and maturation equations are as follows:

$$R_E(t) = b(t)A(t), \tag{5}$$

$$M_E(t) = R_L(t) = R_E(t-\tau_E(t))S_E(t)\frac{g_E(T(t))}{g_E(T(t-\tau_E(t)))}, \tag{6}$$

$$M_L(t) = R_P(t) = R_L(t-\tau_L(t))S_L(t)\frac{g_L(T(t))}{g_L(T(t-\tau_L(t)))}, \tag{7}$$

$$M_P(t) = R_A(t) = R_P(t-\tau_P(t))S_P(t)\frac{g_P(T(t))}{g_P(T(t-\tau_P(t)))}, \tag{8}$$

where $b(t)$ represents the rate adult mosquitoes lay eggs, $\tau_i(t)$ represents the variable stage duration of an individual, $S_i(t)$ represents the through-stage survival rate of individuals, and $g_i(T(t))$ represents the temperature-dependent development rate of individuals during stage i (where $i = E, L, P$). The ratio $\frac{g_i(T(t))}{g_i(T(t-\tau_i(t)))}$ is the relative growth rate of individuals, where when $\frac{g_i(T(t))}{g_i(T(t-\tau_i(t)))} > 1$ development rate is faster, and when $\frac{g_i(T(t))}{g_i(T(t-\tau_i(t)))} < 1$ development rate is slower than at the beginning of the corresponding stage i (where $i = E, L, P$).

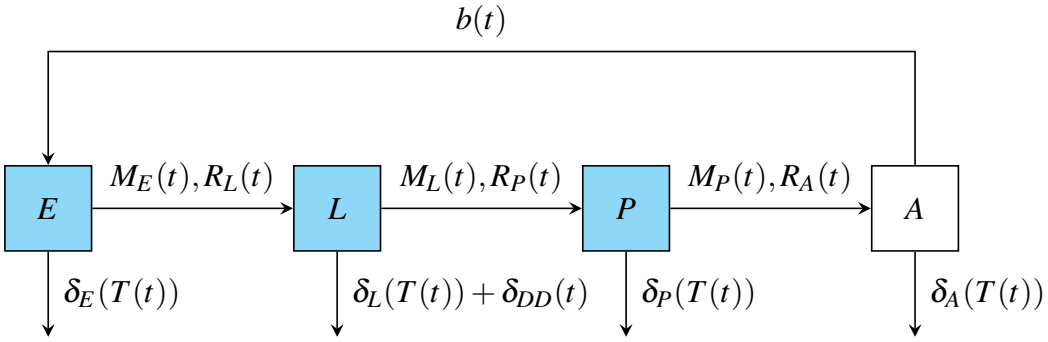

Figure 3: Schematic of the life cycle model framework. Adults (A) lay eggs (E) at a rate $b(t)$, which either mature $M_E(t)$ or die at a rate $\delta_E(T(t))$. After, maturation eggs are recruited into the larvae (L) stage $R_L(t)$ where they either mature into pupae $M_L(t)$, die at a rate $\delta_L(T(t))$ or die due to density-dependence $\delta_{DD}(t)$. After maturation they are recruited into the pupae (P) stage $R_P(t)$ where they either mature $M_P(t)$ or die at a rate $\delta_P(T(t))$, from which they are then recruited into the adult stage $R_A(t)$ and lay eggs again or die at a rate $\delta_A(T(t))$. Classes that are coloured blue represent the aquatic stages.

The equations describing the delay in stage duration $(\tau_i(t))$ and gonotrophic cycle $(G(T(t)))$ are as follows:

$$\frac{d\tau_E(t)}{dt} = 1 - \frac{g_E(T(t))}{g_E(T(t-\tau_E(t)))}, \tag{9}$$

$$\frac{d\tau_L(t)}{dt} = 1 - \frac{g_L(T(t))}{g_L(T(t-\tau_L(t)))}, \tag{10}$$

$$\frac{d\tau_P(t)}{dt} = 1 - \frac{g_P(T(t))}{g_P(T(t-\tau_P(t)))}, \tag{11}$$

$$\frac{d\tau_G(t)}{dt} = 1 - \frac{g_G(T(t))}{g_G(T(t-\tau_G(t)))}. \tag{12}$$

Where, $\tau_i(t)$ is the development time given that the development of stage i is completed at time t, $g_i(t)$ is the development rate when development is complete, and $t - \tau_i(t)$ is the time when individuals enter the development stage.

The equations describing the through-stage survival rates for each life stage are as follows:

$$\frac{dS_E(t)}{dt} = S_E(t)\left[\frac{\delta_E(T(t-\tau_E(t)))g_E(T(t))}{g_E(T(t-\tau_E(t)))} - \delta_E(T(t))\right], \tag{13}$$

$$\frac{dS_L(t)}{dt} = S_L(t)\left[\frac{\Big(\delta_L(T(t-\tau_L(t))) + \delta_{DD}(t-\tau_L(t))\Big)g_L(T(t))}{g_L(T(t-\tau_L(t)))} - \Big(\delta_L(T(t)) + \delta_{DD}(t)\Big)\right], \tag{14}$$

$$\frac{dS_P(t)}{dt} = S_P(t)\left[\frac{\delta_P(T(t)-\tau_P(t)))g_P(T(t))}{g_P(T(t-\tau_P(t)))} - \delta_P(T(t))\right]. \tag{15}$$

Where $S_i(t)$ is the proportion of individuals that survive life stage i, calculated by the cumulative mortality rate $\delta_i(t)$ during each individual life stage i ($i = E, L, P$).

2.2 Model Parameterisation

2.2.1 *Anopheles* Mosquito Life History Traits

The model was parameterised using thermal performance curves to describe temperature-dependent processes occurring during each life stage. Here temperature at any given time

t is denoted by $T(t)$, and for simplicity it is assumed there is no difference between air and water temperature. A literature search was carried out in order to obtain published data for the temperature-dependent processes such as development rate $g(T(t))$, survival $\hat{S}(T(t))$ (described in more detail below), and gonotrophic cycle length $g_G(T(t))$ for female *Anopheles gambiae* mosquitoes. Thermal performance curves were fit to the data using non-linear least squares (NLS) in R using the rTPC package [63]. R^2 values for each curve were assessed to determine the best fit function to the data for each life history trait.

Eggs

Recruitment into the egg stage relies upon the completion of the gonotrophic cycle $g_G(T(t))$. The birth rate at time t is therefore defined as

$$b(t) = \frac{1}{2}\left[\frac{n_E}{g_G(T(t))}\right], \tag{16}$$

where n_E denotes the number of eggs laid by a female mosquito, per gonotrophic cycle. Table 1 provides this and all the parameter values and their sources. As the aim is to model female mosquito population dynamics, the birth rate here is halved under the assumption of a 1:1 sex ratio.

Although frequently assumed constant, multiple studies [3,6] have shown that the gonotrophic cycle is temperature-dependent and can vary in duration up to two days with minor fluctuations in temperature. To capture these variations five studies that investigate the temperature influences on the duration of the gonotrophic cycle have been used due to limited data availability for a single species. Four laboratory studies evaluate the duration of the gonotrophic cycle of *Anopheles gambiae* at temperatures ranging from $21 - 31°C$ [2–5]. These temperatures are typical for areas where *Anopheles gambiae* are present and therefore relevant for the case study of this model. As these studies did not measure variation near the temperature extremes, we supplement this with data from Lardeux et al. (2008) [6] for *Anopheles pseudopunctipennis*, that measured the duration of the gonotrophic cycle at temperatures ranging from $10 - 35°C$. The latter dataset has been used in previous studies as a proxy for other *Anopheles* mosquito species due to the lack of available data [52]. Here, it is assumed that

the gonotrophic cycle is the duration of time from blood meal to egg laying. As these experiments were carried out in the laboratory, there is no effect of blood meal availability, and the time taken to seek a host is neglected and assumed to be instantaneous. The data from these studies was combined in order to fit the thermal performance curve for the gonotrophic cycle process (Figure 4). The best fitting functional form explaining the duration of the gonotrophic cycle was the Brière function given by:

$$g_G(T(t)) = \theta_1 T(t)(T(t) - \theta_2)(\theta_3 - T(t))^{\frac{1}{\theta_4}}. \tag{17}$$

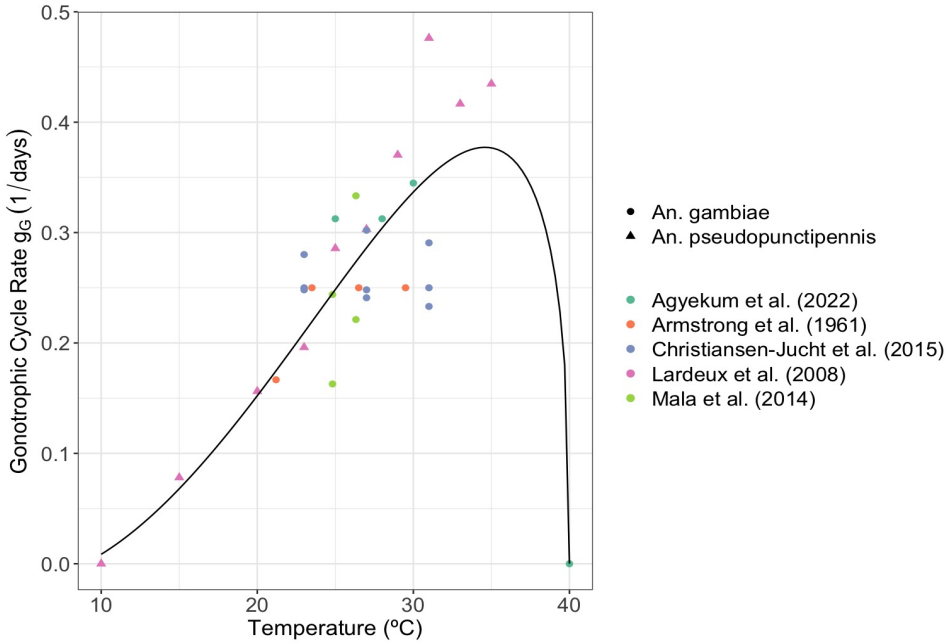

Figure 4: Thermal performance of the gonotrophic cycle. Each point represents the duration of the gonotrophic cycle at a specific temperature, and the points are coloured corresponding to which study the data came from [2–6]. The shape of the points represents the corresponding species. A Brière function was fitted to the dataset giving $R^2 = 0.844$

To parameterise the egg development rate, data obtained by digitalising results from Bayoh (2001) [7] was used. This was the only data available for egg development for *Anopheles gambiae* species, and was best explained by the Gaussian functional form (Figure 5A) defined by

$$g_E(T(t)) = \alpha_{1_E} \exp\left(-\frac{1}{2}\left[\frac{T(t) - \sigma_{1_E}}{\gamma_{1_E}} \right]^2 \right). \tag{18}$$

Anopheles gambiae egg survival data was unavailable, therefore data pertaining to the survival of *Anopheles arabiensis* from a study carried out by Maharaj et al. (2003) [8] was used as a substitute. Here, egg survival is denoted as $\hat{S}_E(T(t))$ which represents the temperature-dependent proportion of eggs that survive to next life stage, which allows for the estimation of the mortality rate. This does not equate to $S_E(t)$ which is the through-stage survival rate of individuals at time t. The best fitting functional form was the Gaussian function (Figure 5B) defined by:

$$\hat{S}_E(T(t)) = \alpha_{2_E} \exp\left(-\frac{1}{2}\left[\frac{T(t) - \sigma_{2_E}}{\gamma_{2_E}} \right]^2 \right). \tag{19}$$

The mortality rate at a given time t, is defined by

$$\delta_E(t) = \frac{-\log(\hat{S}_E(T(t)))}{\tau_E(T(t))}. \tag{20}$$

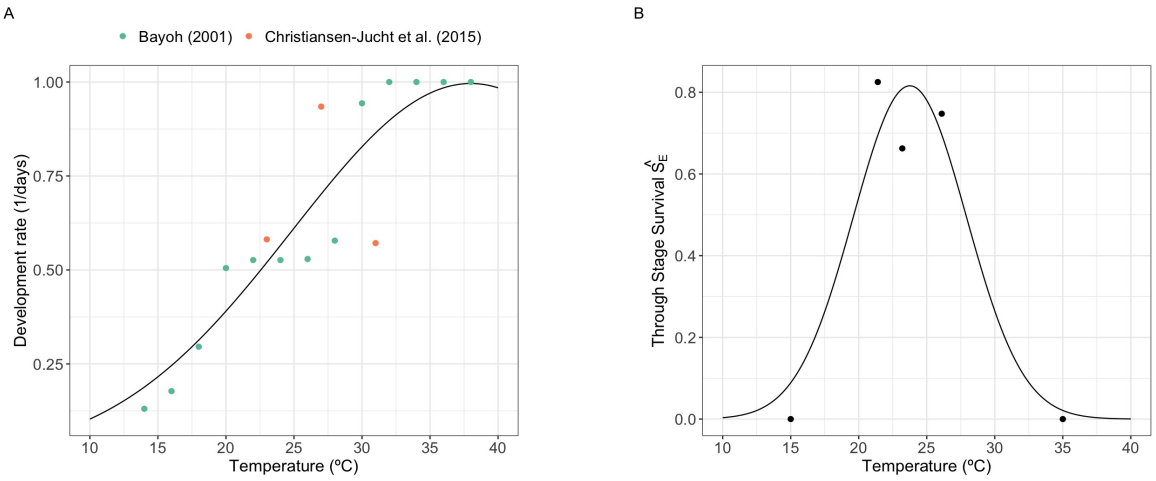

Figure 5: Thermal performance of egg development and through-stage survival over a temperature range $10 - 40°C$. **A:** Gaussian function fit to *Anopheles gambiae* development data from [7] with $R^2 = 0.823$ **B:** Gaussian function fit to *Anopheles arabiensis* data from [8] with $R^2 = 0.929$.

Larvae

Mosquito larvae go through multiple processes during the larval stage. The life history processes during this stage are not only influenced by temperature-dependent development and survival, but also density-dependence.

Data pertaining to the development of mosquito larvae at different temperatures was taken from the same study as the egg data [7, 38]. Although data for development rate of each larvae instar is available, because the equivalent for larvae survival is not, the larvae stage was simplified and modelled as a single stage. At temperatures $10-16^{\circ}$C and $34-40^{\circ}$C larvae did not survive beyond the second instar stage, and therefore no development data was used at these temperatures. This was combined with data taken from a later study carried out by Barreaux et al. [9] who measured larval development time at three temperatures $(21, 25, 29^{\circ}\text{C})$. The best fit for total larvae development rate was a Gaussian function (Figure 6A) defined by:

$$g_L(T(t)) = \alpha_{1_L} \exp\left(-\frac{1}{2}\left[\frac{T(t)-\sigma_{1_L}}{\gamma_{1_L}}\right]^2\right). \tag{21}$$

Data exploring larvae survival was used from three studies [2, 7, 10], and was measured as the percentage of larvae that pupate. The best fit to this data was a Gaussian function (Figure 6B) and defined by:

$$\hat{S}_L(T(t)) = \alpha_{2_L} \exp\left(-\frac{1}{2}\left[\frac{T(t)-\sigma_{2_L}}{\gamma_{2_L}}\right]^2\right). \tag{22}$$

As described above for the egg mortality, the same process applies here and therefore the temperature-dependent mortality rate at time t is given by:

$$\delta_L(t) = \frac{-\log(\hat{S}_L(T(t)))}{\tau_L(T(t))}. \tag{23}$$

Another very important process in *Anopheles* mosquito population dynamics is density-dependence and competition during the aquatic stage. Here it is assumed that density-dependence only impacts larvae survival, and occurs in the form of excess mortality due to competition which is regulated by habitat availability. Other processes such as canabalism and predation from other species is also present during this stage however due to data availability and simplicity this is not accounted for here.

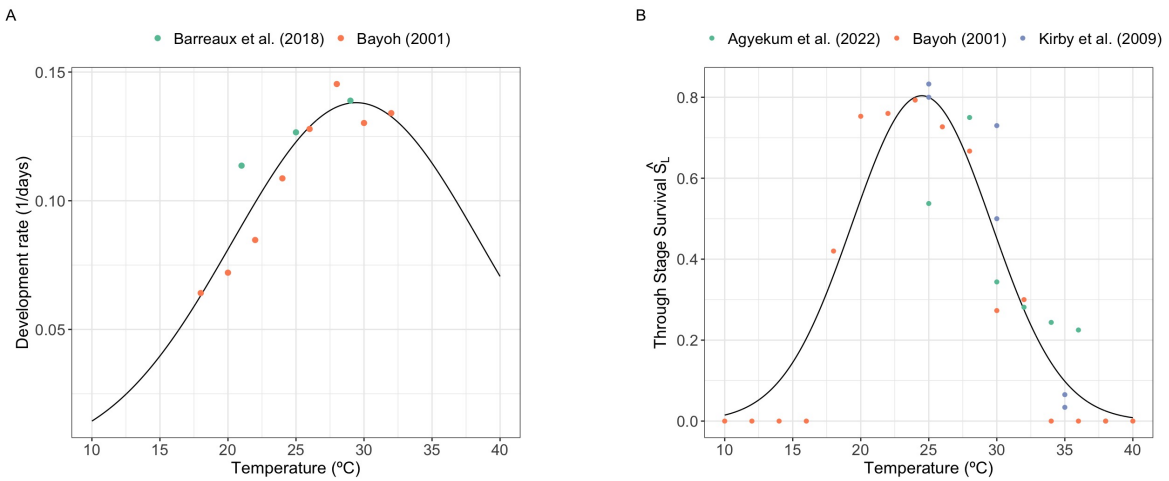

Figure 6: Thermal performance of larvae development and through-stage survival at a temperature range of $10-40^{\circ}C$. **A:** Gaussian function fit to *Anopheles gambiae* development data from [7,9] with $R^2 = 0.865$ **B:** Gaussian function fit to data from [2,7,10] with $R^2 = 0.869$.

Studies that measure density-dependence are limited. However, Njunwa et al. (1993) measured daily larval mortality at densities 20, 50 , 100, 200, 300 larvae/16cm^2 [27]. They found a linear relationship between larval mortality and density, such that;

$$\delta_L(T(t)) + \delta_{DD}(t)L(t) = c_0 + c_1 L. \tag{24}$$

Here c_0 accounts for the density-independent mortality, and c_1 is the rate of increase in mortality with increasing larval density. The experiment was conducted under semi-field conditions, and carried out over a period of months from January 1990 - December 1991, experiencing fluctuating temperatures with an average of $27^{\circ}C$. Temperatures were reported as monthly averages and variations between months were small.

Using equation (23), at $27^{\circ}C$ $\delta_L(T(t)) = 0.0501$, and in the experiment $c_0 = 0.056$. As the value for $\delta_L(T(t))$ falls within the confidence interval of the c_0 value from the original study, it is assumed that there is no interaction between temperature and density, such that $\delta_{DD}(t)L = c_1 L$, and when habitat is available, c_1 describes the strength of density-dependent competition.

In the experiments, there was 100% habitat available throughout and rainfall was not a factor as the experiments were conducted under a canopy, however in general habitat availability varies seasonally with rainfall [64]. To adjust for this, it is assumed that strength of competition decreases proportionally with habitat size, which is modelled as,

$$\delta_{DD}(t)L(t) = \frac{c_1 L}{W(t)}, \tag{25}$$

where $W(t)$ is the amount of habitat available per km^2 at time t. $W(t)$ refers to both temporary habitats ($w_{temp}(t)$), such as small pools and puddles, and permanent habitats (w_{perm}), such as rice fields and large irrigated areas which exist all year round. Here it is assumed that the maximum amount of habitat per km^2 is 4% in line with Tompkins et al. [11]. It is also assumed that during the dry season there is a baseline amount of permanent habitat constantly available in order to maintain the mosquito population.

$$W(t) = w_{temp}(t) + w_{perm}. \tag{26}$$

A description of the methods used to model $w_{temp}(t)$ is described in Section 2.2.2.

Pupae

Pupae development and survival data was taken from the same study [7, 38]. Development time was defined as the number of days it takes pupae to become adults, and survival was defined as the proportion of pupae that successfully become adults. The best fit for the development was the Gaussian function (Figure 7A):

$$g_P(T(t)) = \alpha_{1_P} \exp\left(-\frac{1}{2}\left[\frac{T(t) - \sigma_{1_P}}{\gamma_{1_P}} \right]^2 \right), \tag{27}$$

and the best fit for pupae survival was also the Gaussian function (Figure 7B):

$$\hat{S}_P(T) = \alpha_{2_P} \exp\left(-\frac{1}{2}\left[\frac{T - \sigma_{2_P}}{\gamma_{2_P}} \right]^2 \right). \tag{28}$$

As described above in the egg and larvae mortality, the same process applies here and therefore the temperature-dependent mortality rate at time t for pupae is given by:

$$\delta_P(t) = \frac{-\log(\hat{S}_P(T(t)))}{\tau_P(T(t))}. \tag{29}$$

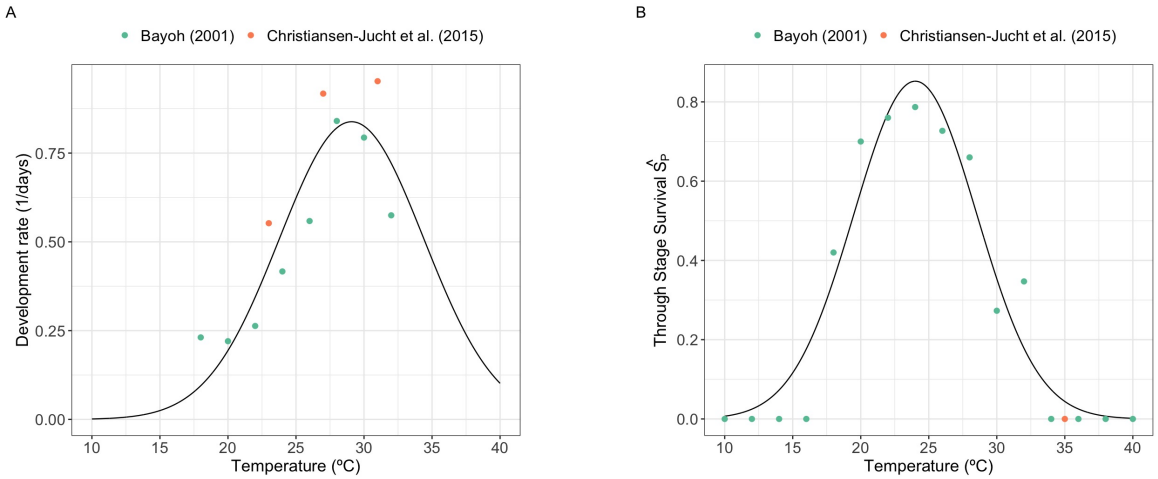

Figure 7: Thermal performance of pupae development and through-stage survival at temperature range $10-40°C$. **A:** Gaussian function fit to *Anopheles gambiae* development data from [7] with $R^2 = 0.806$, **B:** Gaussian function fit to data from [7] with $R^2 = 0.935$.

Adults

Adult survival is defined as the average number of days it takes for 50% of adults to die off, and was taken from a study carried out by Bayoh (2001) [7]. Here, it is assumed that humidity is constant throughout at 60%, however as this dataset evaluated survival at varying temperatures at constant humidity levels of 40, 60, 80, and 100%, it allows the model's sensitivity to different humidity levels to be tested. The best fit to the data was the Gaussian function (Figure 8),

$$\hat{S}_{A_x}(T(t)) = \alpha_{A_x} exp\left(-\frac{1}{2}\left[\frac{T(t) - \sigma_{A_x}}{\gamma_{A_x}} \right]^2 \right), \tag{30}$$

The adult mortality rate is then determined by:

$$\delta_A(t) = \frac{\ln(2)}{\hat{S}_{A_x}(t)}. \tag{31}$$

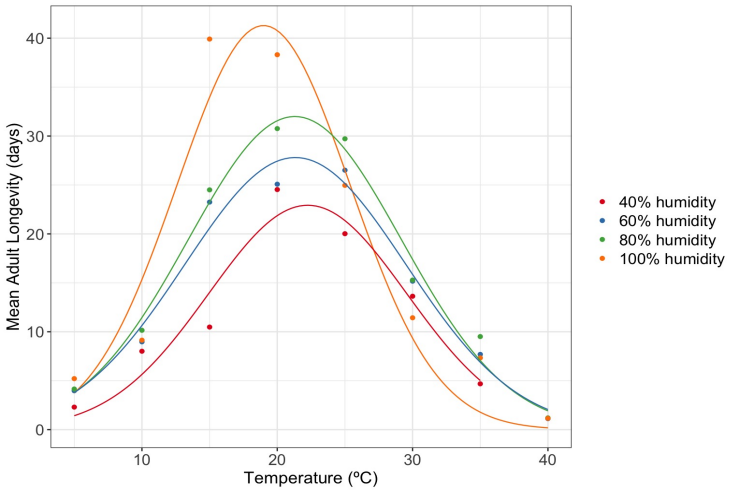

Figure 8: Thermal performance of adult longevity at temperature range $10-40°C$, and humidity levels $40-100\%$. Data for *Anopheles gambiae* taken from [7] was used for the fitting, with a Gaussian function fit to data at each humidity level. Each coloured point and line represent the observed data and corresponding reaction norm, respectively, at each level of humidity.

2.2.2 Habitat Availability (w_{temp})

Larvae survival is strongly influenced by the amount of habitat available in the environment, as this regulates the strength of competition for space and food. As mentioned, *Anopheles gambiae* prefer temporary habitats that are formed by rainfall. Therefore, a process is required in order to predict the amount of habitat that would be available at any given point in time, driven by the dynamics of the environment. In this study, temporary habitats are defined as small rain-fed pools that do not exist year round. These habitats are formed when rain falls into a ground depression resulting in an accumulation of water, which is then used as larvae habitat (see Figure 9).

In a given area (here a km^2 grid cell), there is a maximum amount of area that has the potential to become habitat for mosquito larvae (w_{max}), and at any given point in time t a fraction of this is viable habitat (w_{temp}). This fraction of available habitat consists of multiple pools of varying size and shape. These pools are created when precipitation falls directly into the ground depressions ($R(t)$). This precipitation can either fall directly on the current water available, or fall on the remainder of the area inside the depression that does not yet contribute to the surface area. A fraction of this water then can also feed the pool generated as surface run-off (R_{frac}). When $R_{frac} = 0$ any water that falls into the depression that is not on the current surface is lost into the soil and does not contribute to the growth of the habitat. When $R_{frac} = 1$, all water that falls into the depressions, regardless if it is directly onto the current surface area or not will contribute to the habitat growth. There is

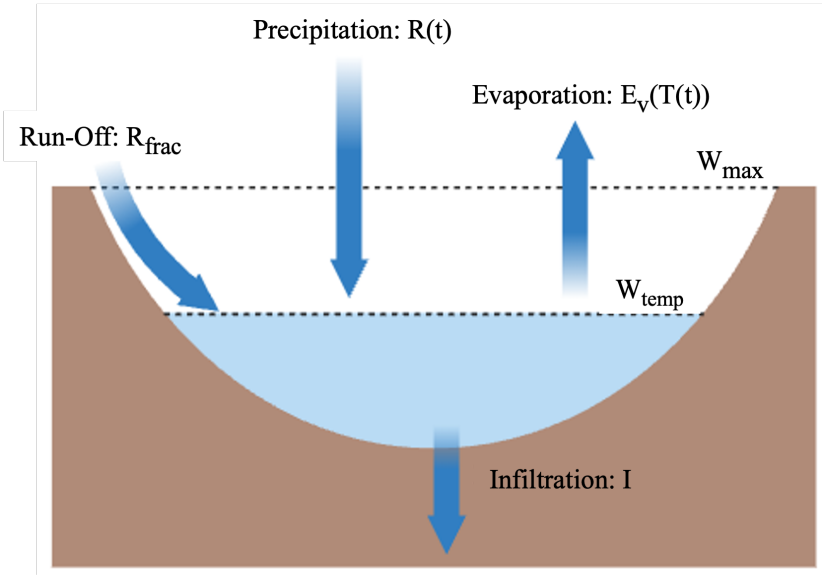

Figure 9: Schematic of the processes involved in the formation of a viable habitat. Water fills a ground depression by precipitation falling directly onto the surface area $A(t)$, or falling on the area inside the depression yet to be covered by water which a fraction of then contributes to the filling of the site R_{frac}. Water is lost through evaporation $E_v(T(t))$ and infiltration into the soil I. The maximum the site can reach is w_{max}. Blue arrows correspond to the water gain/loss in the site.

also water loss through infiltration (I) and evaporation ($E_v(T(t))$) which here is calculated using Hamon's equation:

$$e_s(T(t)) = 0.6108 \exp\left(\frac{17.27T(t)}{T(t)+237.3}\right), \tag{32}$$

$$E_v(T(t)) = 2.1H_r^2\left(\frac{e_s}{T(t)+273.3}\right). \tag{33}$$

Where, $e_s(T(t))$ is the evaporation saturation which is dependent on temperature, T is temperature at time t, and H_r is the hours of daylight.

In order to model these processes, a simple water-balance model is used that explains the rate of change in temporary water coverage:

$$\frac{dw_{temp}}{dt} = \lambda\left[R(t)(w_{temp} - R_{frac}(w_{max} - w_{temp})) - w_{temp}(E_v(T(t)) + I)\right]. \tag{34}$$

The λ parameter is used to relate the rate of change in volume to the growth of that habitat. Here two modelling approaches are considered; 1) A model developed by Tompkins et al. [11] (hereon referred to as Tompkins Model) that assumes a linear relationship between rainfall and the growth of the habitat, which is set as a constant parameter and 2) A model presented by Eikenberry et al. [12] (hereon referred to as the Eikenberry Model) which relates the volume of the habitat to surface area based on the physical properties of the site, which changes at each time step.

Another difference between these modelling approaches is that the Tompkins Model calculates the total fractional coverage of temporary habitat available, and they incorporate an overflow term into the model which balances out the scenario where if there are habitats that are different sizes, when some are at their maximum others may still be filling up. They assume this relationship to be linear. They also assume that all water that falls into the depressions contribute to the growth of the site and therefore set $R_{frac} = 1$. In the case of the Tompkins Model, equation (35) becomes:

$$\frac{dw_{temp}}{dt} = \lambda \left[R(t)(w_{temp} - R_{frac}(w_{max} - w_{temp})) \left(1 - \frac{w_{temp}}{w_{max}}\right) - w_{temp}(E_v(T(t)) + I) \right], \quad (35)$$

where λ is a constant value and $\left(1 - \frac{w_{temp}}{w_{max}}\right)$ accounts for overflow from varying habitat size.

Alternatively, the Eikenberry Model models a single habitat that explicitly uses the geometry of the site to relate water volume to the area of temporary habitat available such that;

$$\lambda = \frac{2}{p h_{max}} \left(\frac{w_{max}}{w_{temp}} \right)^{\frac{p}{2}}, \quad (36)$$

where h_{max} is the height of the water in the depression, and p is a dimensionless parameter that describes the shape of the depression. As the Eikenberry Model does not model the total fraction of habitat and instead models a single depression that is then scaled up to account for all temporary habitat in the given area, it does not require an overflow term and therefore the Eikenberry Model is equivalent to equation (35) with λ substituted with equation (37).

Table 1: Table of parameter values used in model

Parameter	Description	Value (3 dpt)	Reference
$\alpha_{A_{60}}$	Maximum adult survival (60% humidity)	27.804 days	[7]
$\sigma_{A_{60}}$	Optimal temperature for adult survival (60% humidity)	$21.335°C$	[7]
$\gamma_{A_{60}}$	Adult survival coefficient (60% humidity)	8.177	[7]
θ_1	Gonotrophic cycle coefficient	0.0001	[3, 6]
θ_2	Lower temperature gonotrophic cycle threshold	$9.106°C$	[3, 6]
θ_3	Upper temperature gonotrophic cycle threshold	$40°C$	[3, 6]
θ_4	Gonotrophic cycle coefficient	1.535	[3, 6]
n_E	Number of eggs laid by adult female	175	[23]
α_{1_E}	Maximum egg development rate	0.996	[7, 38]
σ_{1_E}	Optimal temperature for egg development	$38°C$	[7, 38]
γ_{1_E}	Egg development coefficient	13.152	[7, 38]
α_{1_L}	Maximum larvae development rate	0.138	[7, 38]
σ_{1_L}	Optimal temperature for larvae development	$29.422°C$	[7, 38]
γ_{1_L}	Larvae development coefficient	9.132	[7, 38]
α_{1_P}	Maximum pupae development rate	0.838	[7, 38]
σ_{1_P}	Optimal temperature for pupae development	$29.088°C$	[7, 38]
γ_{1_P}	Pupae development coefficient	5.312	[7, 38]
α_{2_E}	Maximum egg survival rate	0.816	[8]
σ_{2_E}	Optimal temperature for egg survival	$23.758°C$	[8]
γ_{2_E}	Egg survival coefficient	4.159	[8]
α_{2_L}	Maximum larvae survival rate	0.804	[7, 39]
σ_{2_L}	Optimal temperature for larvae survival	$24.491°C$	[7, 39]
γ_{2_L}	Larvae survival coefficient	5.127	[7, 39]
α_{2_P}	Maximum pupae survival rate	0.852	[7, 39]
σ_{2_P}	Optimal temperature for pupae survival	$24.012°C$	[7, 39]
γ_{2_P}	Pupae survival coefficient	5.312	[7, 39]
c_1	Strength of larvae competition	0.002	[46]
w_{perm}	Minimum fractional coverage of permanent habitat	10^{-6}	[11]
$w_{\max}$	Maximum potential temporary habitat coverage	0.04 km^2	[11]
λ	Scaling factor	1/1000	[11]
H_r	Hours of daylight	12	[47]
I	Infiltration	245 mm/day	[11]
A_{max}	Maximum area of temporary habitat	3.8m^2	[54]
h_{max}	Maximum depth of temporary habitat	120 mm	[54]
p	Shape parameter of temporary habitat	1	[54]

2.3 Numerical Simulations

Model simulations were carried out using Julia software using the DifferentialEquations package [65], and were simulated with daily time steps. As the model consists of delay-differential equations, initial history must be provided i.e. when time $t < 0$. Here the initial conditions for equations (1) - (4) are set as $E = L = P = A = 0$, and temperature as the first recorded temperature of the environmental dataset. Using the temperature value when $t < 0$, can then determine the initial values for equations (9) - (16). The system is started by an

initial inoculation of 10 adults when $t = 1$. The model uses environmental data for two years prior to the desired time series required as a burn-in period. The Tompkins model for habitat was solved in R using the deSolve package [66], and the Eikenberry habitat model was simulated in MATLAB using the ode15s solver.

2.4 Validation of Population Dynamics Model

To check that the model correctly predicts patterns in mosquito abundance, the model must first be validated against previous data. For this long-term field surveillance data from a village in Burkina Faso from 2018-2023, and from a village in the Garki District in Nigeria ranging from 1971-1973 was taken. This was carried out in R, where predictions and observed data were normalised by the maximum abundance across the time series. Model accuracy was evaluated using the R^2 value as a goodness of fit measure.

2.4.1 Burkina Faso

Long term adult mosquito abundance surveillance data from a village, Tengrela, was collected via human landing traps during 2018-2023 (inclusive) by the Centre National du Research et de Formation sur le Paludism (CNRFP; unpublished). Daily regional data from the Banfora weather station was combined with village specific monthly weather data from WorldClim database.

Collections were carried out monthly in two households, each with two traps, one indoor and one outdoor. Here the data is not aggregated by location and therefore the indoor and outdoor collections are combined. After each trapping event, all mosquitoes were counted and morphologically speciated. For the purpose of this study, abundance counts pertaining to *Anopheles gambiae* caught per night per trap were used to make trapping event comparable in case of failed or missing traps.

Tengrela is located $\sim$ 10 km from Banfora in Burkina Faso. The mosquito habitat in the area is comprised mainly of temporary rain-fed pools and puddles, however there is also a permanent swamp as well as a large lake close by. The village has a variable climate with the dry season typically between November-March, and the wet season April-October. P2.0 treated bed nets were deployed in the village until the beginning of 2020, when they were replaced by upgraded IG2 nets.

2.4.2 Nigeria

Long-term adult mosquito data from the Garki District of Nigeria, was collected from 1971-1973 (inclusive) as part of the Garki Project [62]. When available, corresponding temperature and rainfall was also collated for the corresponding village during the project. Discrepancies and missing entries were supplemented by satellite data collected from NOAA. As data for the specific villages was unavailable, the closest weather station (Kano, located $\sim$ 80 km south-west of Garki) was selected. This data was directly substituted in to the village datasets.

2.5 Field Surveillance Data from Burkina Faso

Entomological surveillance data from a step-wedge cluster Randomised Control Trial (cRCT) was collected from the Cascades region of Burkina Faso. This trial was conducted as part of the AvecNet project [13], and hereafter is referred to as the AvecNet trial. The objective of this trial was to compare effectiveness of a novel Insecticide Treated Net (OlysetDUO) that combines a pyrethroid insecticide with an insect growth regulator (pyriproxyfen) to a standard pyrethroid-only net (Olyset). This trial was carried out over a period of two years (2014-2016) in 40 geographic clusters drawn from 81 villages. The OlysetDUO nets were introduced in a phased approach with village clusters receiving them at different times over the course of the two year trial.

To investigate the population dynamics of *Anopheles gambiae* mosquitoes in the Banfora region of Burkina Faso, data from a singular cluster is taken as an example for the model simulation. Specifically, data from cluster 25 from 2014-2015 was used. As the model does not account for the impact of interventions, this cluster and time period were chosen because it provides data from a full season prior to the deployment of the new OlysetDUO nets. The data consisted of monthly human landing catches from two households, which was complemented by weather data as described above in Section 2.4.

3 Results

3.1 Evaluating the Changes in Shape and Size of Temporary Habitat Models

In this section, the shape and size of different aquatic habitat models will be evaluated, and how the difference for habitat availability and timing of each model will be explored, separately. These are explored when precipitation is constant through each of the wet and dry seasons (100 and 0mm, respectively). The consequences of the different temporary aquatic habitats for population dynamics will be assessed in the subsequent section (Section 3.2), in the context of validation.

3.1.1 Tompkins Model

The main processes influencing the dynamics of this model are the fractional run-off as well as the λ parameter which translates the volume of a pool to the surface area i.e., the fractional coverage of habitat per km^2.

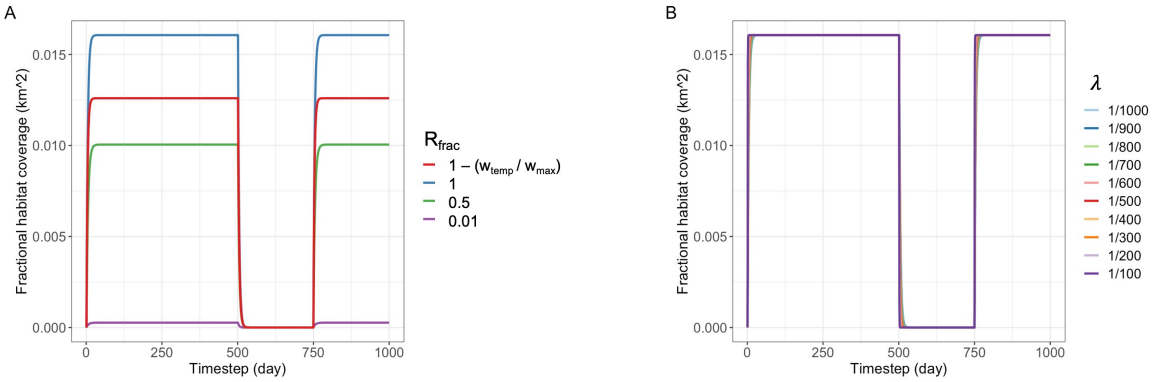

Figure 10: Fractional habitat coverage under continuous rainfall conditions of Tompkins model [11] **A:** when R_{frac} is varying with each coloured line representing a different condition, and **B:** when λ varies from $1/100 - 1/1000$ where each coloured line represents a different value. Where no rainfall occurred between day 500-750, otherwise rainfall $R(t) = 100$ mm to represent the dry and wet season, respectively and parameters as shown in Table 1.

First testing the scenario of variation in R_{frac}, four scenarios were evaluated; $R_{frac} = (1 - \frac{w_{temp}}{w_{max}})$ which assumes that run-off decreases linearly with area, $R_{frac} = 1$ (default value), $R_{frac} = 0.5$, and $R_{frac} = 0.01$. Figure 10A shows that as the fraction of run-off that contributes to habitat growth decreases, the amount of surface area available also decreases. This is to be expected as there is less water contributing to habitat growth and more loss. Figure 10A also shows that the lower the amount of run-off the longer it takes for the pools to fill. Conversely, when R_{frac} is lower, the pool empties more quickly compared to when a

higher ratio of R_{frac} is contributing to the growth of the pools.

Figure 10B depicts scenarios for when λ is varying. In the habitat model, λ is the variable relating the volume of water to the area coverage. In the Tompkins Model this is set as a constant with a value of 1/1000 [11]. Here, a range of values for λ were tested ranging from 1/1000 - 1/100. Figure 10B shows that as the value of λ affects the start and end of season accumulation. When $\lambda = 1/100$, these processes happen almost instantaneously taking only one day, however when $\lambda = 1/1000$, this takes considerably longer to empty, resulting in small values of λ converting rainfall into area at a lower rate than when λ is large.

3.1.2 Eikenberry Model

The features of this model that have the greatest influence on the water dynamics are the proportion of run-off contributing to water accumulation R_{frac}, the shape of the habitat p, and the depth of the habitat h_{max}. To assess the influence of these mechanisms, the model is simulated with constant precipitation and evaporation (Figure 11).

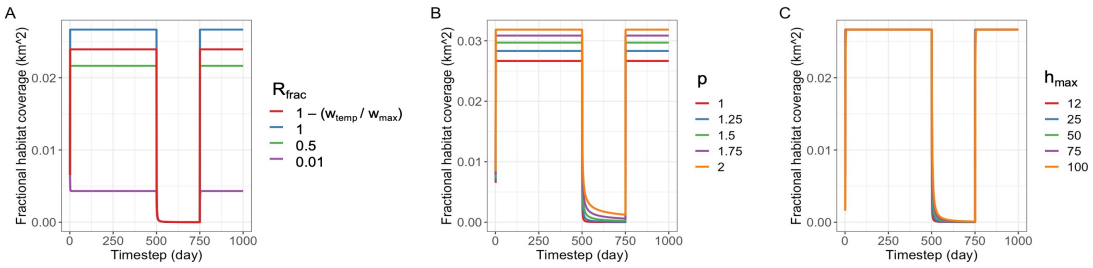

Figure 11: Fractional habitat coverage under continuous rainfall conditions of Eikenberry model [12] **A:** when R_{frac} is varying with each coloured line representing a different condition, **B:** when p is varied from $1-2$ where each coloured line represents a different value, and **C:** when h_{max} is varied from $12-100$. Where no rainfall occurred between day 500-750, otherwise rainfall $R(t) = 100$ mm to represent the dry and wet season, respectively and parameters as shown in Table 1.

Assessing the influence of the amount of run-off that contributes to habitat growth R_{frac}. Figure 11A, shows similarly to the Tompkins model as run-off decreases the coverage of habitat also decreases. Unlike the Tompkins model however, a key difference here is that regardless of the proportion of run-off that contributes to habitat growth, there is no variation in the duration of time taken for habitat to fill or empty.

Another key parameter in this model is the shape parameter p. This controls the geometry of the habitat, typically ranging between 1-2 [54], and here a range of values for p are tested at 0.25 intervals. Figure 11B shows that as p increases the time taken for the habitat to empty significantly increases. In the scenario where $p > 1.5$ the habitat does not fully empty prior

to beginning of the second simulated wet season, which means there is a sustained amount of habitat during the dry season which has a duration of 250 days. This suggests that $p \leq 1.5$ is more realistic for temporary habitats.

Lastly, the depth of the habitat (h_{max}) is evaluated at a range of values. Here the default value is set at 120mm [54], and then scenarios where h_{max} ranges from 250-1000mm are tested. Figure 11C shows that the deeper the pool the longer it takes to dry out at the end of the wet season, however there does not appear to be much variation in the time taken to fill the habitats.

3.2 Population Dynamics Model Validation

Model validation was used to determine the most appropriate habitat model by evaluating the predictive ability of each scenario above, with the observed data from Burkina Faso and the Garki Project. Environmental data for each location is input into the population dynamics model, and the prediction is then compared to the observed data. Model accuracy is assessed using the R^2 metric. There were 10 available datasets, however two will be presented here (Tengrela, Burkina Faso and Village 3 from the Garki Project) for illustrative purposes. These two villages were chosen to demonstrate the generalisability of the model as they represent very distinct populations, with different pressures.

3.2.1 Tengrela, Burkina Faso

Tengrela experiences strong seasonality with clearly defined wet and dry seasons (Figure 12). Figure 12A shows that the highest observed temperatures typically occur at the beginning of the wet season. Temperatures generally fall within the range $23 - 34°C$ year round, with the exception during the 2020 dry season where it falls to $21°C$.

Figure 12B and 12C show the habitat coverage area for the Eikenberry and Tompkins models, respectively. Figure 12B shows that the Eikenberry model consistently generates more habitat peaking $> 0.02\text{km}^2$, compared with the Tompkins model (Figure 12C), which peaks $\approx 0.005\text{km}^2$.

Across both the Eikenberry and Tompkins model seasonality is well captured, however the timing of the start of the wet season, and the speed at which the population disappears during

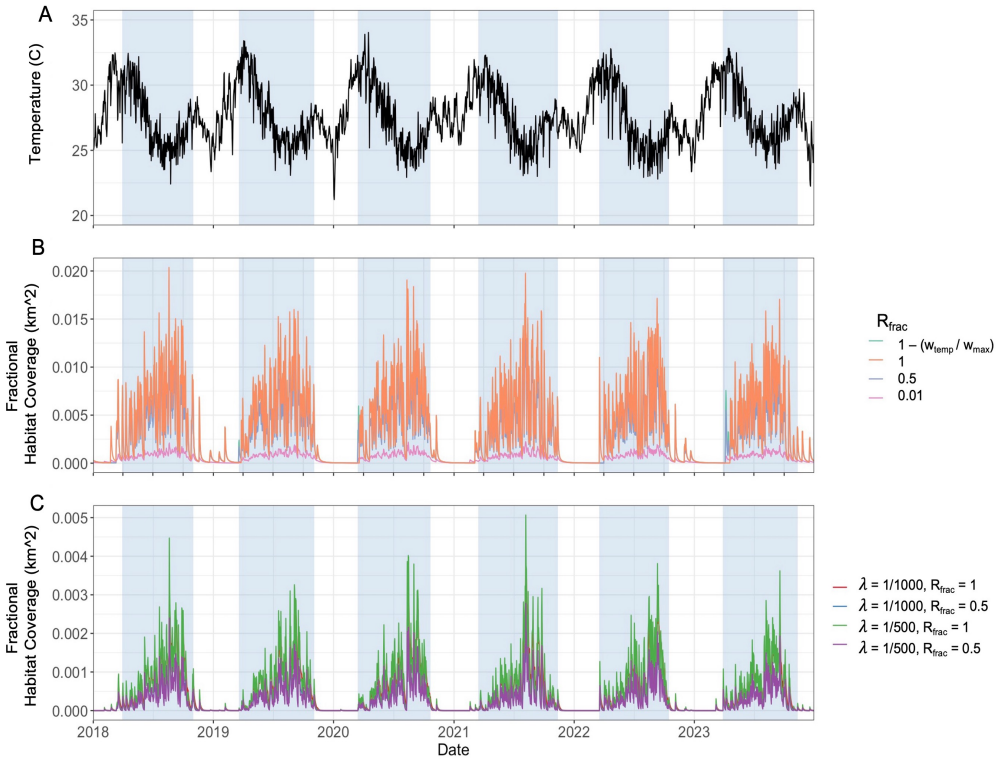

Figure 12: Environmental Conditions, Tengrela. Each panel shows environmental data from 2018-2023 for **A:** Temperature, **B:** Habitat coverage generated by Eikenberry model where each coloured line represents a different run-off model, **C:** Habitat coverage generated by the Tompkins model where each coloured line represents a different combination of λ and R_{frac}.

the wet to dry season transition, was variable year to year. This led to shorter predicted dry seasons compared to the observed data.

Figure 13 shows the predicted adult and larvae population dynamics, and larvae survival using the Tompkins habitat model. In the majority of scenarios, there were only small changes in the population dynamics, with $\lambda = 1/500$ and $R_{frac} = 1$ having the most impact with lower larvae populations sizes (Figure 13A) that does not seem to be reflected in adult population sizes (Figure 13C). These discrepancies between larvae and adult populations could possibly be due to larvae survival (Figure 13B) associated with density-dependence increases.

All variations of the Eikenberry model performed less well compared to the Tompkins model against the Tengrela dataset. This is visible in the model fit (Figure 14). Figure 14A shows that larvae abundances are much higher, this means that the habitat reaches its carrying capacity earlier, as seen by very low levels of larvae survival (Figure 14B) from the middle of the wet season onwards. This is in contrast with the Tompkins model, where larvae survival continues to peak throughout the wet season (Figure 13B). In the Eikenberry model however, there is a significant amount of habitat available (Figure 12B) and therefore this translates

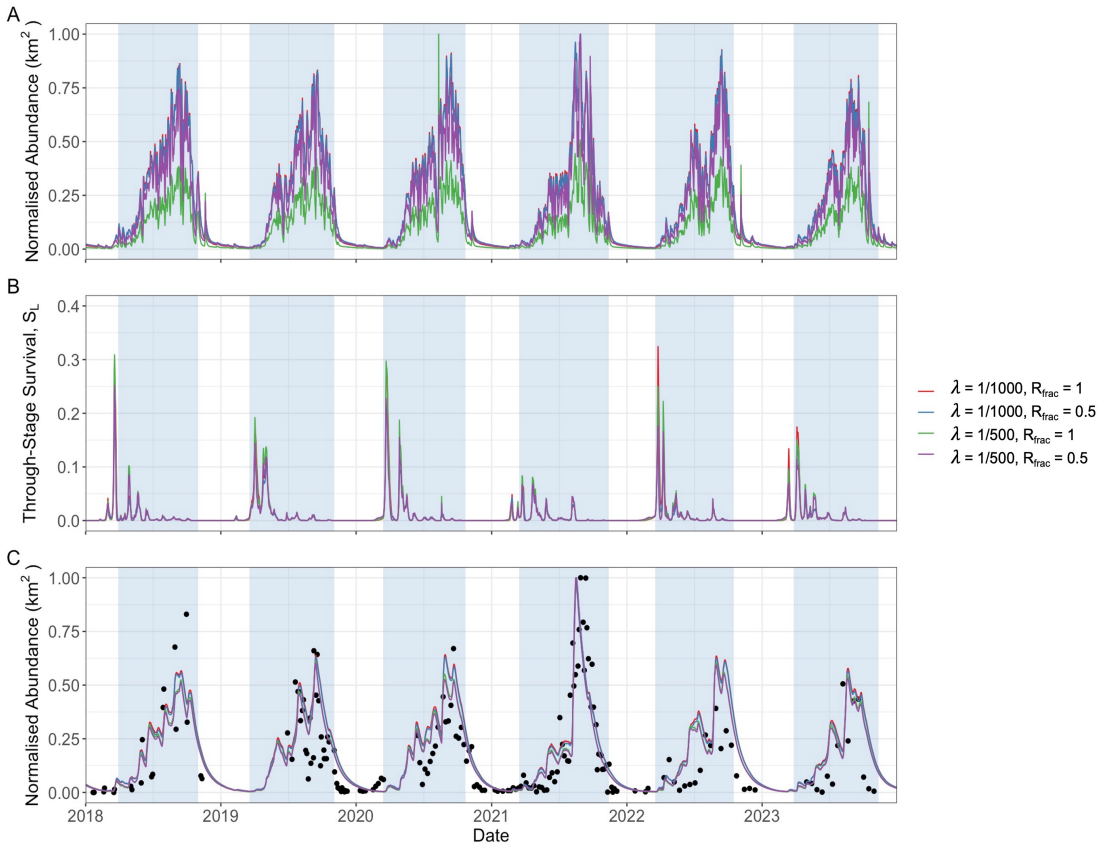

Figure 13: Population dynamics of female mosquito population in Tengrela, Burkina Faso, from 2018-2023 using the Tompkins habitat model. Each coloured line represents a different combination of λ and R_{frac}, and transparent blue panels depict the wet season. **A:** normalised larvae abundance per km^2, **B:** larvae survival, **C:** normalised female adult mosquito abundance where coloured lines are the model prediction and black points are unpublished observed data.

to higher abundance of larvae and adults late into the dry season (Figures 14A and 14B). Generally, there is not significant variation in normalised adult abundance across all run-off scenarios, however when $R_{frac} = 1 - w_{temp}/w_{max}$ (linear relationship) the population appears to start earlier than in the other cases. This seems to fit the data better in certain years, such as 2020 and 2022, however not in 2021 with little influence to the end of the season.

Table 2: Values of R^2 for Tompkins and Eikenberry model in Tengrela, Burkina Faso.

Tompkins Model	R^2
$\lambda = 1/1000, R_{frac} = 1$	0.616
$\lambda = 1/1000, R_{frac} = 0.5$	0.619
$\lambda = 1/500, R_{frac} = 1$	0.62
$\lambda = 1/500, R_{frac} = 0.5$	0.624
Eikenberry Model	R^2
$R_{frac} = 1 - \frac{w}{w_{max}}$	0.469
$R_{frac} = 1$	0.477
$R_{frac} = 0.5$	0.485
$R_{frac} = 0.01$	0.514

To evaluate the model performance compared with observed data, 1-1 plots were used to

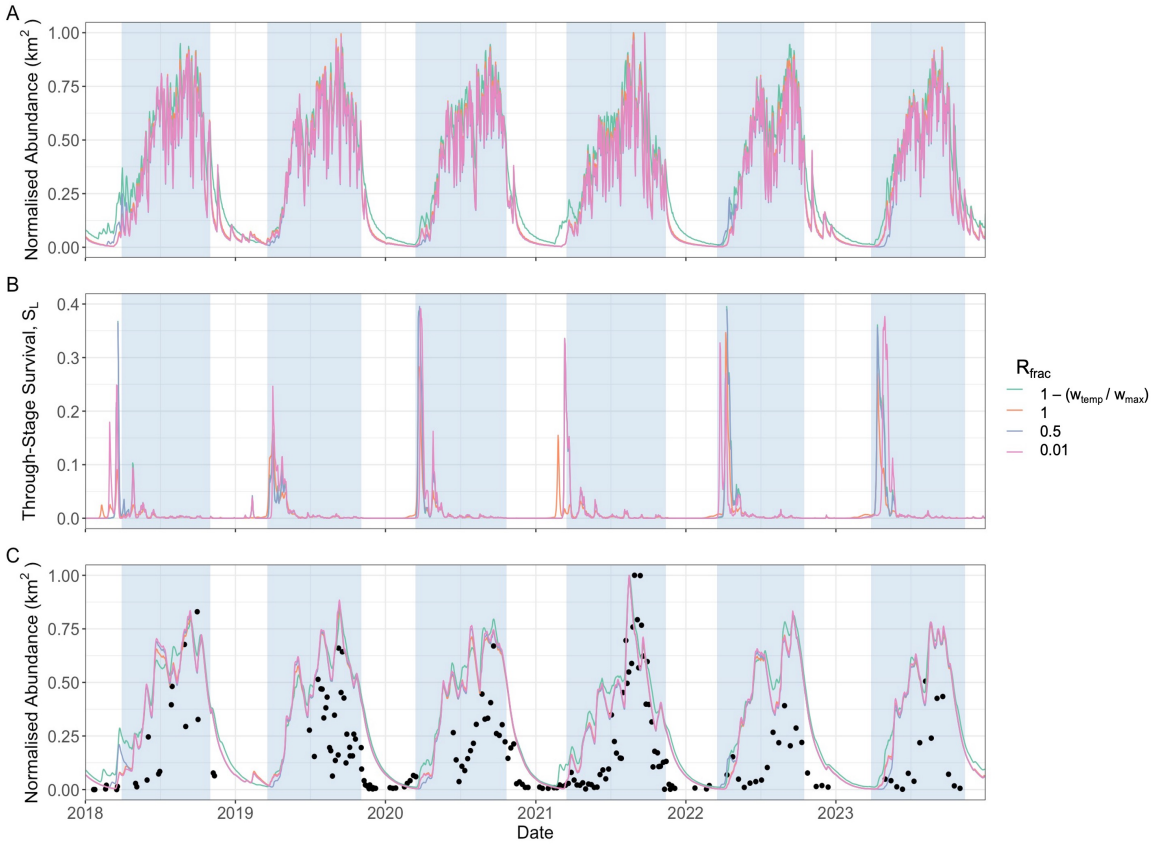

Figure 14: Population dynamics of female mosquito population in Tengrela Burkina Faso over time series 2018-2023 using the Eikenberry model for habitat. Each coloured line represents a different combination of R_{frac}, and transparent blue panels depict the wet season. **A:** normalised larvae abundance per km^2, **B:** larvae survival, **C:** normalised female adult mosquito abundance where coloured lines are the model prediction and black points are unpublished observed data.

check where most of the variation occurs (Figures 15 and 16). Table 2 shows that the R^2 values are very similar across all Tompkins model scenarios, however there is much more variation in the Eikenberry model fits. The best performing population dynamics model where habitat is calculated using the Tompkins model is the case where $\lambda = 1/500$ and $R_{frac} = 0.5$. From Figure 15 it can also be seen that generally the model always overestimates the dry season abundance, however, underestimates normalised adult abundance when observed data is at its peak. In Figure 16, more generally the Eikenberry habitat models overestimates the observed population not just during the dry season but also almost always during the wet season except when the observed population is at or near its peak. This suggests that the model is retaining a lot more habitat which is resulting in more mosquito abundance year round, which is a result of λ being much higher, compared to the Tompkins model. Therefore, the conversion from volume to area is smaller and rainfall leads to faster rate of accumulation of area in the Eikenberry model. Table 2 also shows that the goodness of fit of the Eikenberry model is significantly lower than that of the Tompkins model, with the best fit case when run-off is lowest $(R^2 = 0.514)$

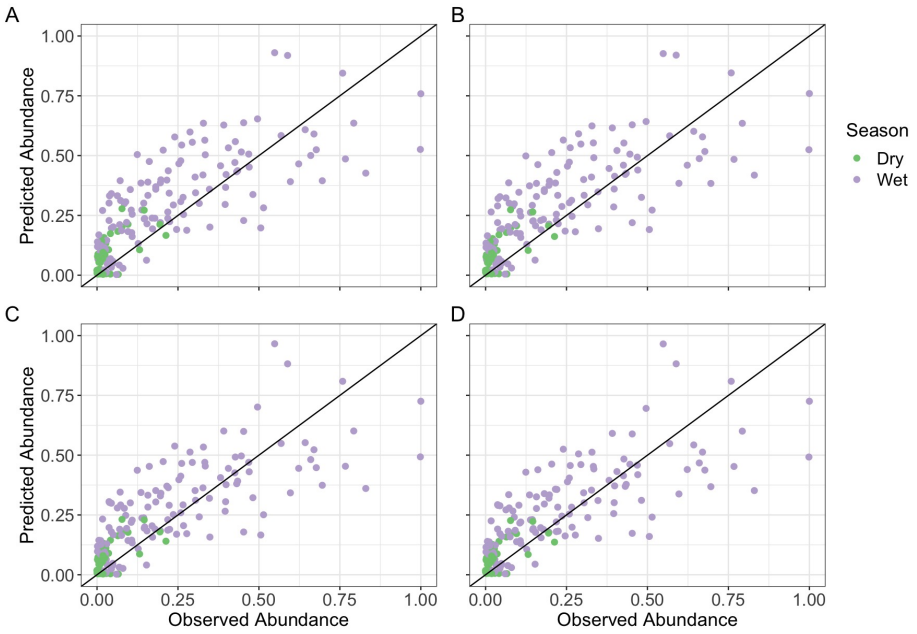

Figure 15: 1-1 ratio plot of model prediction vs observed data in Tengrela, Burkina Faso, from 2018-2023 using the Tompkins habitat model. Points are coloured by season either dry (green) or wet (purple) for each combination of λ and R_{frac}; **A:** $\lambda = 1/1000, R_{frac} = 1$, **B:** $\lambda = 1/1000, R_{frac} = 0.5$, **C:** $\lambda = 1/500, R_{frac} = 1$, and **D:** $\lambda = 1/500, R_{frac} = 0.5$

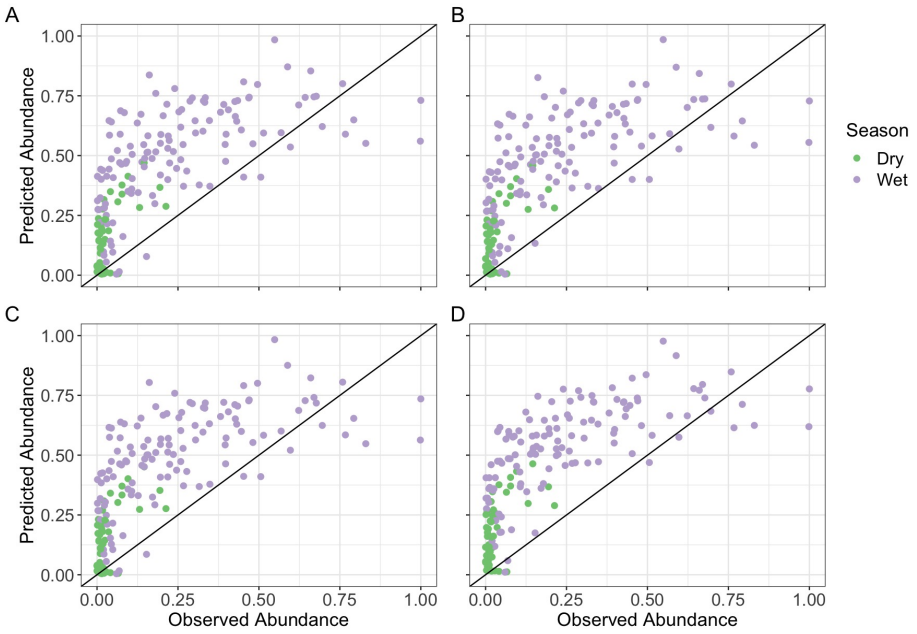

Figure 16: 1-1 ratio plot of model prediction vs observed data in Tengrela Burkina Faso over time series 2018-2023 using the Eikenberry model for habitat. Points are coloured by season either dry (green) or wet (purple) for each combination R_{frac}; **A:** $R_{frac} = 1 - \frac{w}{wmax}$, **B:** $R_{frac} = 1$, **C:** $R_{frac} = 0.5$, and **D:** $R_{frac} = 0.01$

3.2.2 Garki District, Nigeria

Similar to Tengrela (Burkina Faso), the Garki district (Nigeria) also experiences distinct wet and dry seasons. The wet season however is much shorter, with the dry season lasting ≈ 9 months (Figure 17). The temperature in this region is much more diverse, compared to

Tengrela, ranging from $16 - 35°C$ (Figure 17A). Figures 17B and 17C show the temporary habitat predictions for both the Eikenberry and Tompkins models, respectively. In both cases, there is an abundance of habitat throughout the wet season. There are also some pre-peaks in habitat occurring in the dry season (e.g. April 1972), likely due to flash rains causing an accumulation of habitat prior to the commencement of the rainy season.

Although the Garki dataset is shorter (three years) than the Tengrela dataset (six years) the general patterns observed persist, with the Tompkins models generally fitting the data better compared to the Eikenberry model. It is also the same here, where there is a more gradual decline in population at the end of the wet season. This is likely due to the existence of permanent habitat which compared to the temporary habitat, is relatively small, however this becomes crucial in the dry season as it is what sustains the populations.

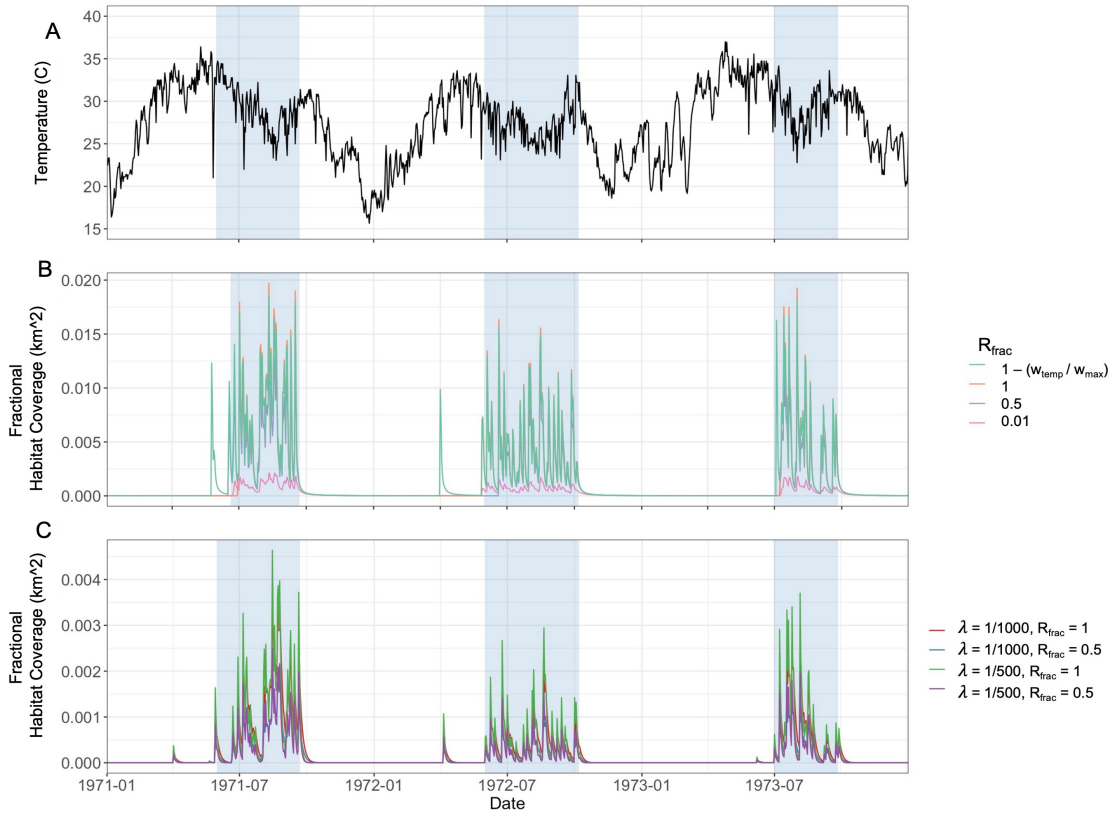

Figure 17: Garki District environmental data from 1971-1973. **A:** Temperature, **B:** Habitat coverage generated by Eikenberry model where each coloured line represents a different run-off model, **C:** Habitat coverage generated by the Tompkins model where each coloured line represents a different combination of λ and R_{frac}.

Figure 18 shows the predicted adundance in the larvae and adult stages, as well as the larval survival when the Tompkins model for temporary habitat is used. Like with the previous dataset, the model fits in all scenarios were similar, however here in the larvae population the highest prediction were in the case where $\lambda = 1/1000$ (Figure 18A). The higher λ values

also produced the highest larvae survival across all years (see Figure 18B), which translated to the adult abundance where the highest peaks were at the highest λ values. Unlike in the Burkina Faso dataset when there were pre-season peaks of habitat using the Tompkins model, this did not translate into abundance peaks in the adult stages, however in the Garki data this does occur. Figure 18C shows that there is a peak in adult abundance during April 1972 which directly coincides with the small peak in larvae population, caused by the spike in available habitat (see Figure 17C). Figure 18C also shows that although across the entire dataset, when $\lambda = 1/500$ and $R_{frac} = 0.5$ produces the maximum R^2 value (see Table 3), during the 1973 wet season, the abundance peak is better captured when using the default set of parameters.

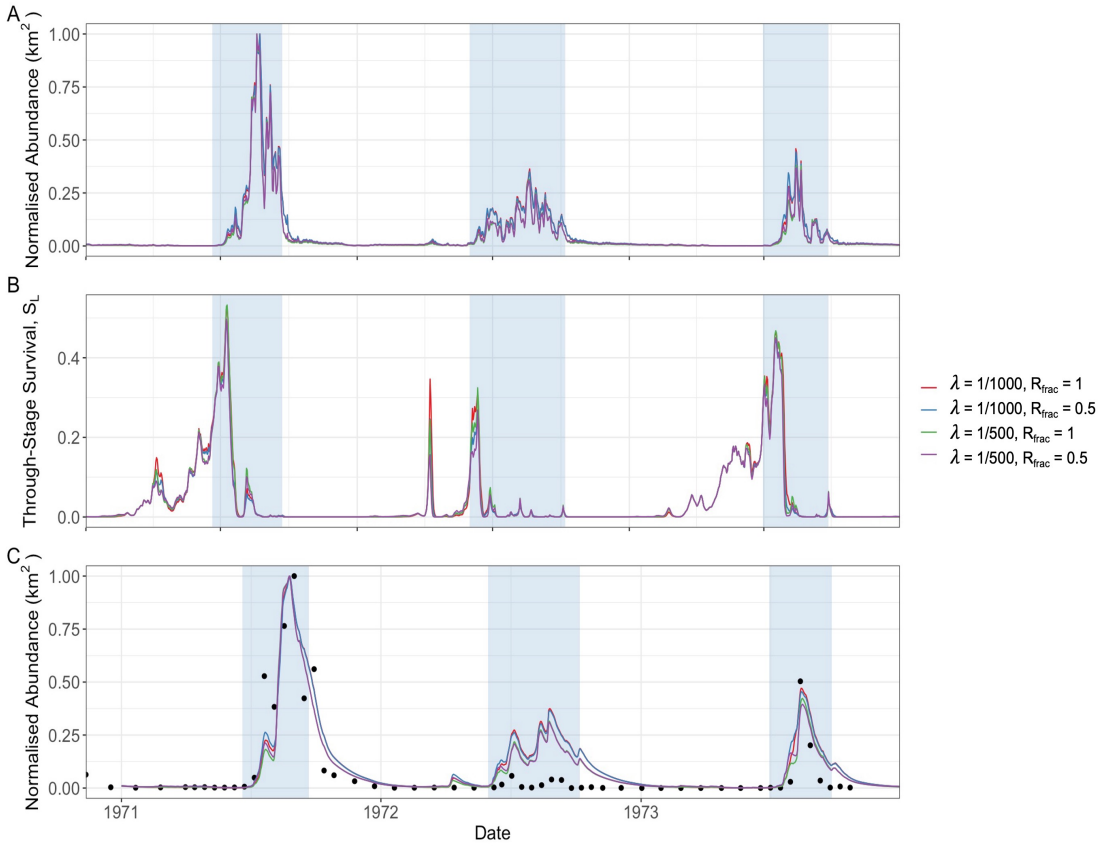

Figure 18: Population dynamics of female mosquito population in Garki District Nigeria (Village 3), from 1971-1973, using the Tompkins habitat model. Each coloured line represents a different combination of λ and R_{frac}, and transparent blue panels depict the wet season. **A:** larvae abundance per km^2, **B:** larvae survival, **C:** female adult mosquito abundance where coloured lines are the model prediction and black points are unpublished observed data.

Figure 19A show that the seasonality of the larvae population dynamics are captured well across the time series, however unlike with the Tompkins model, when $R_{frac} = 1$, the decline in the larvae population is much more gradual with small peaks at the beginning of the dry season. This then creates a more gradual decline in population in the adult abundance (Figure 19C). There is also around one month difference in the peak of the predicted population

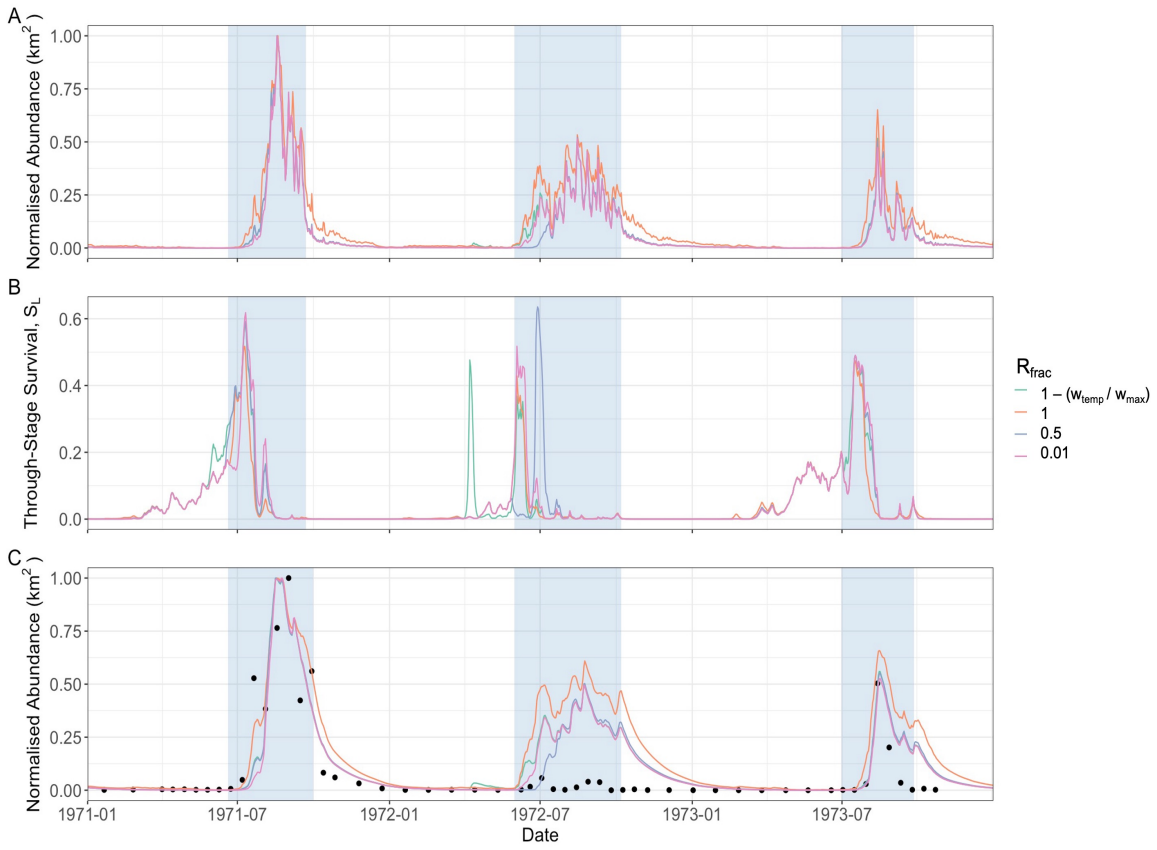

Figure 19: Population dynamics of female mosquito population in Garki District Nigeria over time series 1971-1973 using the Eikenberry model for habitat. Each coloured line represents a different combination of λ and R_{frac}, and transparent blue panels depict the wet season. **A:** larvae abundance per km^2, **B:** larvae survival, **C:** female adult mosquito abundance where coloured lines are the model prediction and black points are unpublished observed data.

Table 3: Values of R^2 for Tompkins and Eikenberry model in Garki District, Nigeria.

Tompkins Model	R^2
$\lambda = 1/1000, R_{frac} = 1$	0.736
$\lambda = 1/1000, R_{frac} = 0.5$	0.752
$\lambda = 1/500, R_{frac} = 1$	0.749
$\lambda = 1/500, R_{frac} = 0.5$	0.761
Eikenberry Model	R^2
$R_{frac} = 1 - \frac{w}{w_{max}}$	0.609
$R_{frac} = 1$	0.584
$R_{frac} = 0.5$	0.607
$R_{frac} = 0.01$	0.525

compared with the field observations. This is significant as the life cycle of the female adult mosquitoes ranges from 10-40 days (Figure 8). The abundance peak during the 1973 wet season is captured well by the Eikenberry model in all scenarios except when $R_{frac} = 1$ where it is overestimated. This is in comparison with the Tompkins model where in each scenario the peak was largely underestimated.

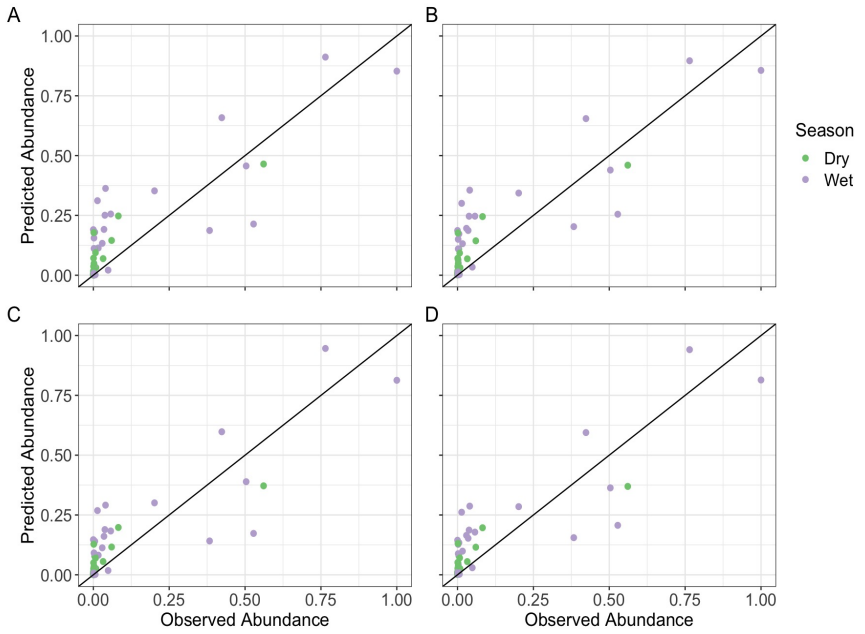

Figure 20: 1-1 ratio plot of model prediction vs observed data in Garki District Nigeria (Village 3), from 1971-1973, using the Tompkins habitat model. Points are coloured by season either dry (green) or wet (purple) for each combination of λ and R_{frac}; **A:** $\lambda = 1/1000, R_{frac} = 1$, **B:** $\lambda = 1/1000, R_{frac} = 0.5$, **C:** $\lambda = 1/500, R_{frac} = 1$, and **D:** $\lambda = 1/500, R_{frac} = 0.5$

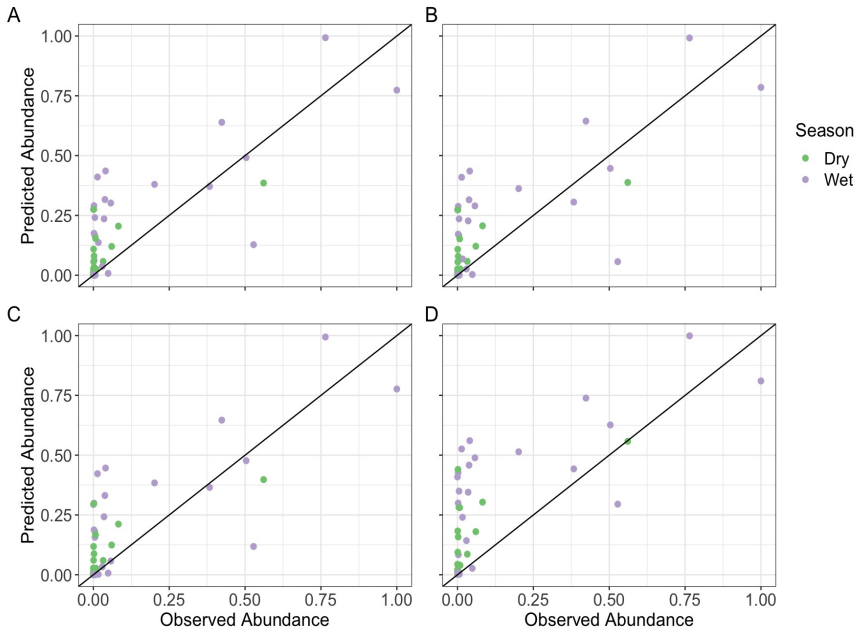

Figure 21: 1-1 ratio plot of model prediction vs observed data in Garki District Nigeria over time series 1971-1973 using the Eikenberry model for habitat. Points are coloured by season either dry (green) or wet (purple) for each combination R_{frac}; **A:** $R_{frac} = 1 - \frac{w}{wmax}$, **B:** $R_{frac} = 1$, **C:** $R_{frac} = 0.5$, and **D:** $R_{frac} = 0.01$

Similarly to the model performance for Burkina Faso, the Tompkins model overestimated the dry season mosquito population in all cases (Figure 20), with the best being the case where $\lambda = 1/500, R_{frac} = 0.5$ giving $R^2 = 0.761$ (Table 3). The Eikenberry model is able to predict the beginning of the seasons, however consistently overestimates the transition from wet to

dry season, where the population does not die out until the middle of the season, which is not reflected in the observed data, as seen in Figure 21.

3.3 Population Dynamics of *Anopheles gambiae* in Burkina Faso

In the previous section, it was shown that the Tompkins model for temporary aquatic habitat generated the best model fit to the observed datasets used for validation, where $\lambda = 1/500$ and $R_{frac} = 0.5$ providing the maximum R^2 value across all simulations. The final model was here used to investigate the mosquito population dynamics in a village of the Cascades region of Burkina Faso, as an example of how the model can be utilised.

The model captured the observed dynamics from the pre-intervention period, however after the intervention is implemented the prediction significantly diverges from the observed abundance (Figure 22). The model then allows the estimation of the impact of the intervention to be evaluated. For example, Figure 22 shows that immediately after the intervention, the first major peak in abundance in August 2015 is averted, and the subsequent abundance peaks were also reduced, with an overall relative abundance reduction of 72%.

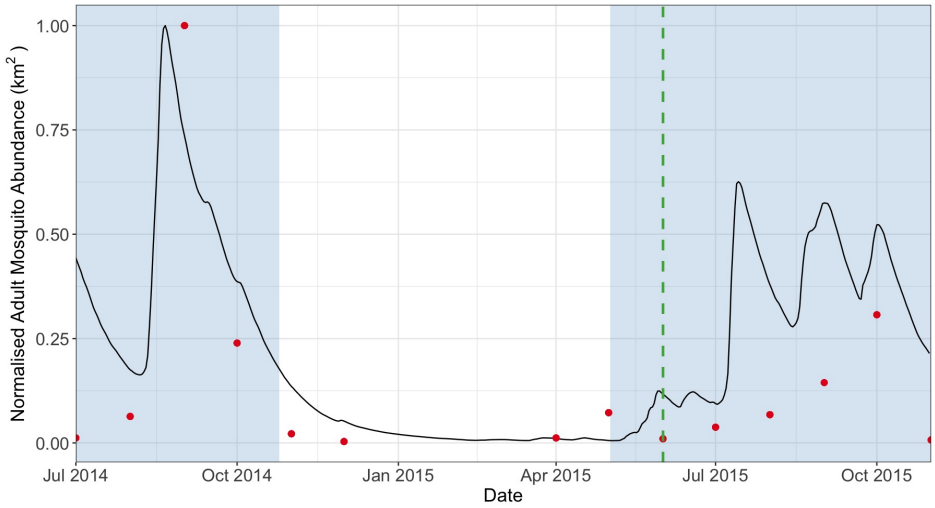

Figure 22: Predicted female mosquito adult abundance in village clusters 21-25 in the AvecNet Trial [13]. The black line is the predicted abundance from the DDE model using the Tompkins temporary habitat model [11], with $\lambda = 1/500$ and $R_{frac} = 0.5$. Each red point is the observed adult abundance in a month, and the green dashed line is when the intervention was introduced. The transparent blue panels highlight the duration of the wet season.

Not only does the model provide insight into the impact of the intervention, it also provides detailed life history trait predictions. Figure 23 shows the prediction of larvae development time, survival, and the duration of the gonotrophic cycle. Given that the aim of this intervention was to target reducing fecundity [13], having a model which is able to track this is

highly informative. I found that larval survival at the beginning of the wet season in 2015 peaks at approximately 0.25, suggesting there are very low levels of density-dependence (Figure 23B). Figure 23C shows that, the peak of the gonotrophic cycle occurs during the middle of the dry season (January 2015), where the highest temperatures are experienced in the area. Having these outputs in particular, are extremely advantageous as mosquito interventions typically target mosquito survival or, in the case of the OlysetDUO nets, fecundity. Having the ability to predict the gonotrophic cycle duration overtime in conjunction with equation (17), gives the user the ability to predict, in the case of the AvecNet trial, what impact this would have on the life history traits.

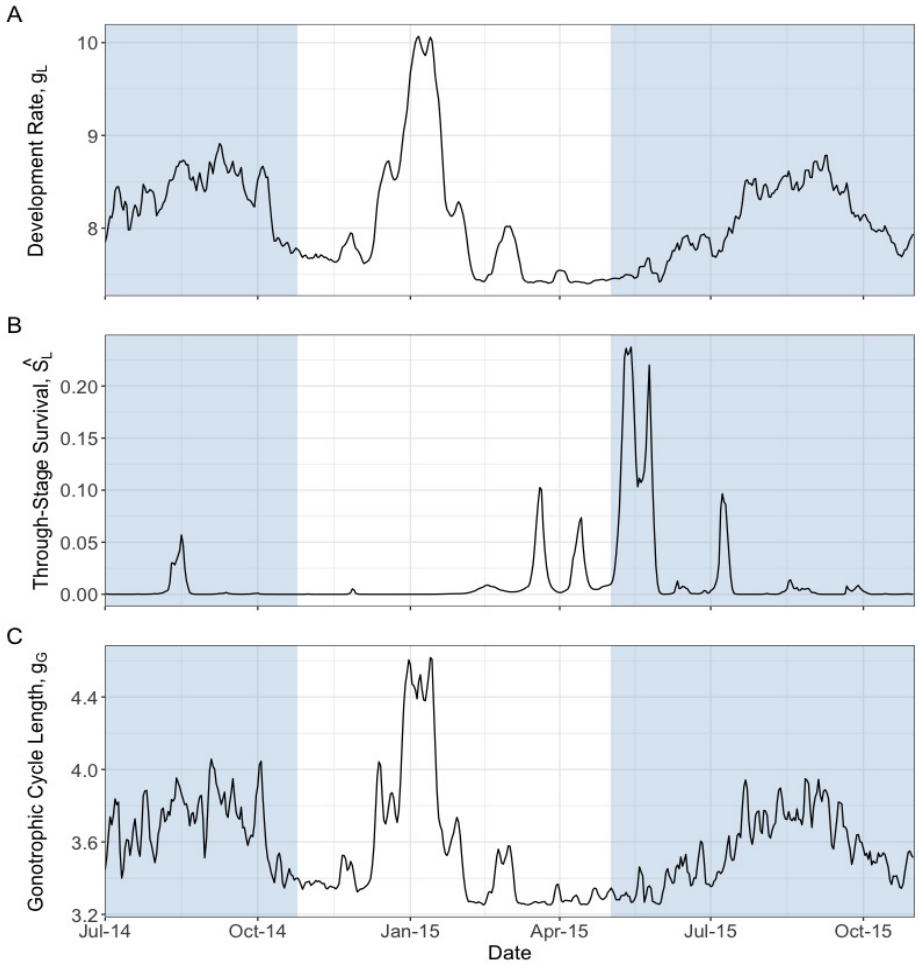

Figure 23: Life-history traits of *Anopheles gambiae* mosquitoes. Transparent blue panels indicate the wet season. Each panel depicts a life history trait **A:** development rate, **B:** through-stage survival, and **C:** duration of the gonotrophic cycle.

More often than not, in mosquito models, traits such as egg and pupae development are assumed to be constant at approximately one day. However, as seen in Figure 24 these processes are much more variable. Figure 24A shows that egg development can reach a maximum of two days, with the longest duration occurring in the dry season. Egg survival also varies considerably, ranging from 0.4-1, with a particular low rate at the beginning of

the wet season (Figure 24B). Similar patterns are reflected in the pupae life history traits (Figures 24C and 24D), with pupae survival at its lowest toward the end of the dry season. These models give important insights into not only the larvae and adult stages (which are the main focus in many modelling studies), but also with the other life stages which are generally less considered. This is important as it allows the consequences of environmental variation to be tracked throughout the entire life cycle of Anopheles *gambiae* mosquitoes.

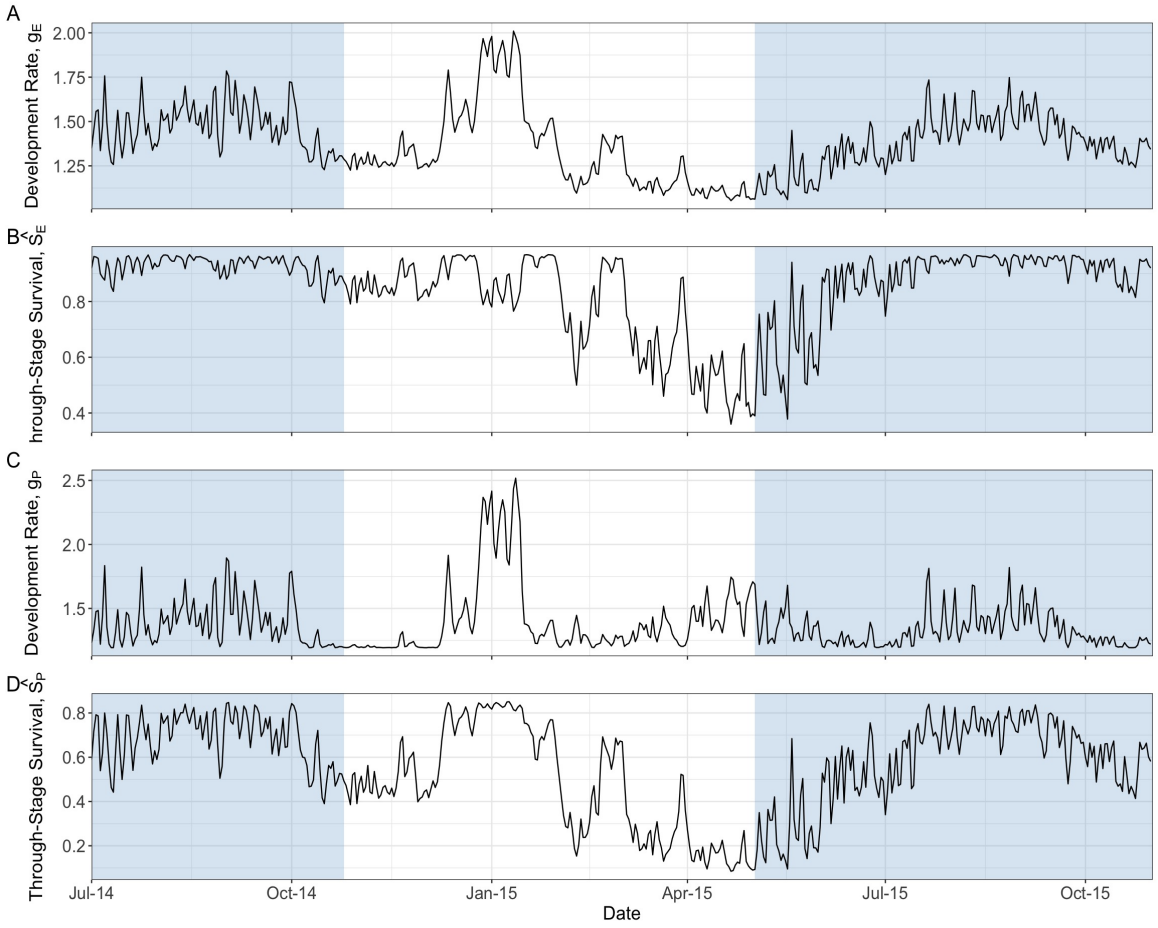

Figure 24: Life-history traits of *Anopheles gambiae* mosquitoes. Transparent blue panels indicate the wet season. Each panel depicts a life history trait **A:** Egg development rate, **B:** Egg through-stage survival, **C:** Pupae development rate, and **D:** Pupae through-stage survival.

4 Discussion

It has long been established that environmental variables such as temperature and rainfall are key drivers in sustaining and influencing mosquito populations, both directly by influencing life history traits, and indirectly by shaping breeding habitat availability [11, 41, 46, 67]. As these are non-linear, complex processes, available population dynamics models have typically focused on single, and often simplified, forms of these processes [46, 48].

In this study, I developed a framework to model the population dynamics of *Anopheles gambiae* mosquitoes, that brings together key environmental factors, namely temperature and rainfall. Specifically, life-history traits such as mosquito development, adult and larvae survival, and gonotrophic cycle duration are included as temperature-dependent processes through thermal performance curves, and density-induced mortality is regulated by the amount of habitat available. Previous studies have taken various approaches to model the effect of rainfall [46, 49, 68], however only a few have considered directly modelling the coverage area of temporary habitats [11, 47, 54]. This is an important ecological factor as it is well known, particularly for *Anopheles gambiae* species, that temporary pools are the preferred habitat [21, 69]. In this model, I compared two approaches for modelling temporary habitats. Firstly, a model developed by Tompkins et al. [11] (Tompkins model), which assumes that the relationship between rainfall and growth of habitat is linear. This model calculates the total fractional coverage of a set area, and takes into consideration variation in habitat size by incorporating an overflow process. Secondly, a model by Eikenberry et al. [12] (Eikenberry model), which instead assumes the physical properties of the individual site such a depth, area, and shape. This model evaluates the change in surface area of a singular habitat using a set of reference values for the physical properties of a habitat. I found that temporary aquatic habitat availability is one of the most influential parameters in these types of model, and that the simplicity of the Tompkins model outperforms the more complex Eikenberry model. This model allowed for the exploratory analysis of the population dynamics in a village in Burkina Faso, highlighting that it could support assessment of interventions.

Anopheles gambiae mosquito populations are highly seasonal, with distinct wet and dry seasons. When compared to validation data, the population dynamics model developed here was able to predict this seasonality, regardless of the habitat model used. Both approaches were also able to estimate the beginning of the wet season. The main challenge was predicting the

dry season, where both models consistently overestimated the mosquito populations. In the field, it is difficult to know for certain what happens to mosquito populations during the dry season, however there are several likely explanations. Abundance is extremely low in the dry season due to lack of standing water, however when the rainy season starts the mosquito populations are extensive [15]. There are several theories on how mosquitoes repopulate after a long period without rain, namely through aestivation, long range migration, or changes in habitat preference [45]. For simplicity here, and due to specific dry season dynamics being unknown, it is assumed that there is always a low level of permanent habitat available. Therefore, as the wet season ends and the simulated habitats dry up, there is a more gradual decline in habitat availability than what would necessarily be observed in the field. Similar approaches have been used in previous studies, for example White et al. [46] assumed that small amounts of the population were able to be detected 20% of the time. There is evidence to suggest that during periods of intense rainfall, larval flushing can occur [42], where some habitats overflow resulting in mosquito larvae being washed out. This was beyond the scope of this study at this stage, and therefore for simplicity this phenomenon was not included here, however this has been accounted for in other studies [11, 47]. Extending the framework to account for flushing, could potentially regulate the larvae population during periods where a significant amount of habitat is available in the wet season. Although there is some evidence of predation and cannibalism occurring in *Anopheles gambiae* mosquito larvae, for simplicity at this stage and due to lack of data availability, this is assumed to be accounted for within the density-dependent mortality through competition. However, if robust data was available to parameterise predation and cannibalism processes during the larvae stage, this could be disentangled and modelled separately from the density-dependent mortality through competition.

A key finding was that the Tompkins model performed better in all validation datasets. In its current form, the Eikenberry model uses reference dimensions of a single habitat which is then scaled up to account for multiple habitats across a given area, essentially modelling multiple copies of the same habitat and assuming uniformity. This is a highly simplifying assumption and, in the field, habitats can be a variety of shapes and sizes [21]. This could be one of the reasons that the Tompkins model performed better, despite its simplicity. The Eikenberry model could be adjusted to account for variation in habitat by categorising habitats by size, and simulating the model with different reference parameters. This variation in the physical properties of the habitats may explain why the Tompkins model does not

produce extreme overestimations in the wet season, as it incorporates an overflow term to account for this. The models were also validated to the overall maximum of the time series, however other options are available (such as normalising per year or to mean value) could change the outcome of how well the predictions fit to the observed data, therefore more exploration is required. Although the Tompkins model performs better than the Eikenberry model, neither are able to capture the end of the wet season properly. This may indicate that there is a mechanism currently missing from the model, or that the traps used for abundance become less efficient at low population sizes. In the datasets from Burkina Faso and the Garki District, the mosquito populations are likely to have been exposed to different vector control efforts and in-turn developed different levels of insecticide resistance that are not directly accounted for in the model or validation. Where possible, an effort to mitigate this effect has been made. For example, while Burkina Faso is known to have high levels of insecticide resistance, it should be minimal in the Garki data as ITNs were not widespread when this data was collected. The AvecNet data was collected during a clinical trial where all houses were given ITNs. While this does not deal with varying levels of insecticide resistance, by choosing villages prior to the implementation of the new intervention, it provides a more stable baseline. Although the results show a good representation of the population dynamics, possible intervention use is likely to contribute to the difference estimated between the predicted dynamics and observed data in the R^2.

Previous models have been used to predict the population dynamics of Anopheline mosquitoes that consider both temperature and rainfall effects, however often make simplifying assumptions regarding these relationships to life history traits. White et al. [46] incorporated temperature dependency into their ODE model, however they assumed a fixed temperature value across all simulations. They also used a different approach to incorporate rainfall-dependency in the carrying capacity, instead opting to integrate cumulative rainfall over time relative to past rainfall events. They validated their model to the Garki project dataset, and also found that their model over estimated the end of the wet season. They were able to improve their model fit when the environmental carrying capacity was exponentially related to the previous rainfall events [46]. Their model was able to predict the observed data better compared to the model presented in this study, however their carrying capacity term involved a tuning parameter which reduces the flexibility in model application to that presented here. Christiansen-Jucht at al. [67] utilised the same exponential carrying capacity into their population dynamics, and applied their population dynamics model to four different scenarios.

Three of those scenarios overestimated the end of the wet season, however they were able to improve their fit to the observed data by incorporating age-structure in the adult stage, something that has not been considered here. In each of these models, the overall seasonality and abundance peaks were captured, however the transition from wet to dry season was consistently overestimated. This further highlights the need for a better understanding of the key processes that drive the decline in the mosquito population at the end of the wet season, which is not well captured by the population dynamics models.

The model presented in this study provides new insights into *Anopheles gambiae* population dynamics. Incorporating delays into the mosquito population model allows for small fluctuations in temperatures throughout the life stages to be accounted for, which traditional models such as ODEs are not able to capture. Although certain Bayesian frameworks could have the capacity to incorporate delay-type processes, it would be more computationally demanding than using delay-differential equations. The model framework developed here also has the potential to be expanded to include intervention impacts. As shown in Section 3.3, the model can be used for counterfactual scenarios of interventions, including the timing of implementation and intensity required. With the incorporation of the habitat model to regulate larvae populations, the model can be used to characterise less known processes such as the time that it takes for aquatic habitats to start producing adults from first rains. This will be important in the context of introducing control measures at the larval stage.

Mosquito population dynamics models, such as the framework developed here, are very data driven. They require a significant amount of data in order to adequately parameterise life history traits. Thermal performance data is required at all life stages, as the mosquito traits are temperature-dependent [4–6, 9, 38, 39], however this type of data is not always available for specific species. For example, the thermal performance of the gonotrophic cycle of *Anopheles gambiae* in each study was only evaluated at a maximum of four temperatures [2–5, 9], and therefore the data had to be supplemented with other species [6]. It is also the case that biologically, the gonotrophic cycle is defined as the time taken for an adult mosquito to find a blood meal and then lay eggs [22, 23]. In laboratory experiments, there is nothing to account for host seeking delays, or the search for a suitable habitat to lay eggs as these are readily available. Therefore, a potential extension to the model could be to account for ecological processes, provided there is available data. The model could be adapted to consider more nuanced dry season dynamics. For example, as there is evidence of

aestivation in *Anopheles* species such as An. *colluzzi* a similar mechanism to that presented by Lehmann et al. [45] could be introduced where mosquitoes become dormant at the end of the rainy season, and the population is then reactivated at the beginning of the wet season, if there is sufficient data available.

In this study R^2 was used as a metric to determine goodness-of-fit of the model prediction to the observed data. Typically R^2 values tend to favour models that contain a higher number of parameters, and therefore could be a limitation of this study. In the comparison between temporary habitat models, in all cases the highest R^2 occurred in the models with fewer parameters (Tompkins model), and therefore the use of R^2 to determine goodness-of-fit is unlikely to have had an impact in this case, however other validation measures could be applied to support findings. The R^2 was also used when comparing thermal performance curves during the model parameterisation stage. Generally, model fits with lower number of parameters generated the highest R^2 and therefore similar to the habitat models the use of this metric is unlikely to have impaired results. The gonotrophic cycle data was best explained by the Brière function which has a higher number of parameters than that of the Gaussian model, however due to the nature of the data (skewed to the right), the Brière function was more appropriate in this instance.

Some advantages of having an advanced modelling framework such as the one presented here, is that the model can be applied at both the local and regional scale. If there is specific knowledge of size and number of breeding sites in a specific location, then the Eikenberry model could be better parameterised for the specific area and may give more accurate predictions in abundance. However, at a regional level if there is little known about specific habitat characteristics, then the Tompkins model is easily applied given it predicts fractional coverage of all habitats, and accounts for variation in size and shape.

In summary, this study has developed a generalisable framework for the population dynamics of *Anopheles gambiae* mosquitoes, and underscores the requirement to incorporate environmental processes. In particular, the exploration of both modelling approaches for temporary habitat has provided unique insight into the key features driving the models, the consequences they have on mosquito population dynamics, and highlights the capability to capture seasonality. This will be important for future work in the context of interventions. Having a model capable of predicting populations at each life stage, as well as individual life history

traits, would allow for a more comprehensive assessment of intervention success, whilst also providing insightful information on targeted approaches to interventions.

References

[1] G. C. Lanzaro and Y. Lee, "Speciation in anopheles gambiae — the distribution of genetic polymorphism and patterns of reproductive isolation among natural populations," in *Anopheles mosquitoes - New insights into malaria vectors* (S. Manguin, ed.), ch. 6, London: IntechOpen, 2013.

[2] T. P. Agyekum, J. Arko-Mensah, P. K. Botwe, J. N. Hogarh, I. Issah, D. Dwomoh, M. K. Billah, S. K. Dadzie, T. G. Robins, and J. N. Fobil, "Effects of elevated temperatures on the growth and development of adult anopheles gambiae (s.l.) (diptera: Culicidae) mosquitoes," *Journal of Medical Entomology*, vol. 59, pp. 1413–1420, 04 2022.

[3] C. D. Christiansen-Jucht, P. E. Parham, A. Saddler, J. C. Koella, and M.-G. Basáñez, "Larval and adult environmental temperatures influence the adult reproductive traits of anopheles gambiae s.s.," *Parasites & Vectors*, vol. 8, no. 1, p. 456, 2015.

[4] J. A. ARMSTRONG and W. R. BRANSBY-WILLIAMS, "The maintenance of a colony of anopheles gambiae, with observations on the effects of changes in temperature. (article) author," *Bulletin World Health Organization*, vol. 24, no. 4-5, pp. 427–435, 1961.

[5] A. O. Mala, L. W. Irungu, E. K. Mitaki, J. I. Shililu, C. M. Mbogo, J. K. Njagi, and J. I. Githure, "Gonotrophic cycle duration, fecundity and parity of anopheles gambiae complex mosquitoes during an extended period of dry weather in a semi arid area in baringo county, kenya," *Int J Mosq Res*, vol. 1, no. 2, pp. 28–34, 2014.

[6] F. J. Lardeux, R. H. Tejerina, V. Quispe, and T. K. Chavez, "A physiological time analysis of the duration of the gonotrophic cycle of anopheles pseudopunctipennis and its implications for malaria transmission in bolivia," *Malaria Journal*, vol. 7, no. 1, p. 141, 2008.

[7] M. N. Bayoh, "Studies on the development and survival of anopheles gambiae sensu stricto at various temperatures and relative humidities," *Durham University*, 2001.

[8] R. Maharaj, "Life table characteristics of anopheles arabiensis (diptera: Culicidae) under simulated seasonal conditions," *Journal of Medical Entomology*, vol. 40, pp. 737–742, 11 2003.

[9] A. M. G. Barreaux, P. Barreaux, K. Thievent, and J. C. Koella, "Larval environment influences vector competence of the malaria mosquito anopheles gambiae.," *Malaria-world J*, vol. 7, p. 8, 2016.

[10] M. J. Kirby and S. W. Lindsay, "Effect of temperature and inter-specific competition on the development and survival of anopheles gambiae sensu stricto and an. arabiensis larvae," *Acta tropica*, vol. 109, no. 2, pp. 118–123, 2009.

[11] A. M. Tompkins and V. Ermert, "A regional-scale, high resolution dynamical malaria model that accounts for population density, climate and surface hydrology," *Malaria Journal*, vol. 12, no. 1, p. 65, 2013.

[12] S. E. Eikenberry and A. B. Gumel, "Mathematical modeling of climate change and malaria transmission dynamics: a historical review," *Journal of Mathematical Biology*, vol. 77, no. 4, pp. 857–933, 2018.

[13] A. B. Tiono, M. Pinder, S. N'Fale, B. Faragher, T. Smith, M. Silkey, H. Ranson, and S. W. Lindsay, "The avecnet trial to assess whether addition of pyriproxyfen, an insect juvenile hormone mimic, to long-lasting insecticidal mosquito nets provides additional protection against clinical malaria over current best practice in an area with pyrethroid-resistant vectors in rural burkina faso: study protocol for a randomised controlled trial," *Trials*, vol. 16, no. 1, p. 113, 2015.

[14] World Health Organization, "Malaria." `https://www.who.int/news-room/fact-sheets/detail/malaria`, March 2023.

[15] N. Becker, D. Petric, M. Zgomba, C. Boase, M. Madon, C. Dahl, and A. Kaiser, *Mosquitoes and their control*. Springer Science and Business Media, 2010.

[16] D. A. Mabayoje and N. Longley, "Malaria and advising the traveller," *Medicine*, vol. 49, no. 12, pp. 774–779, 2021. Infections Part 3 of 3.

[17] WHO, "World malaria report 2025." https://www.who.int/teams/global-malaria-programme/reports/world-malaria-report-2025, 2025.

[18] A. Adeogun, A. S. Babalola, O. O. Okoko, T. Oyeniyi, A. Omotayo, R. T. Izekor, O. Adetunji, A. Olakiigbe, O. Olagundoye, M. Adeleke, C. Ojianwuna, D. Adamu, A. Daskum, J. Musa, O. Sambo, O. Adedayo, P. U. Inyama, L. Samdi, A. Obembe, M. Dogara, P. Kennedy, S. Mohammed, R. Samuel, C. Amajoh, M. Adesola, M. Bala, M. Esema, M. Omo-Eboh, M. Sinka, O. A. Idowu, A. Ande, I. Olayemi, A. Yayo, P. Uhomoibhi, S. Awolola, and B. Salako, "Spatial distribution and ecological niche modeling of geographical spread of anopheles gambiae complex in nigeria using real time data," *Scientific Reports*, vol. 13, no. 1, p. 13679, 2023.

[19] D. Kyalo, P. Amratia, C. W. Mundia, C. M. Mbogo, M. Coetzee, and R. W. Snow, "A geo-coded inventory of anophelines in the afrotropical region south of the sahara: 1898-2016.," *Wellcome Open Res*, vol. 2, p. 57, 2017.

[20] P. Nie, C. He, and J. Feng, "Range dynamics of anopheles mosquitoes in africa suggest a significant increase in the malaria transmission risk.," *Ecol Evol*, vol. 14, p. e70059, Aug 2024.

[21] J. E. Gimnig, M. Ombok, L. Kamau, and W. A. Hawley, "Characteristics of larval anopheline (diptera: Culicidae) habitats in western kenya.," *J Med Entomol*, vol. 38, pp. 282–288, Mar 2001.

[22] J. D. Charlwood, *The Ecology of Malaria Vectors*. Taylor and Francis Group, 2020.

[23] "Anopheles gambiae s.l: morphology, life-cycle, ecology." `https://targetmalaria.org/wp-content/uploads/2020/11/Ecology_FS_EN_Anopheles-gambiae-s.l.-morphology_August20`, August 2020.

[24] J. S. Barr, L. E. Martin, A. T. Tate, and J. F. Hillyer, "Warmer environmental temperature accelerates aging in mosquitoes, decreasing longevity and worsening infection outcomes.," *Immun Ageing*, vol. 21, p. 61, Sep 2024.

[25] R. Bellone and A.-B. Failloux, "The role of temperature in shaping mosquito-borne viruses transmission.," *Front Microbiol*, vol. 11, p. 584846, 2020.

[26] S. M. Muriu, T. Coulson, C. M. Mbogo, and H. C. J. Godfray, "Larval density dependence in anopheles gambiae s.s., the major african vector of malaria.," *J Anim Ecol*, vol. 82, pp. 166–174, Jan 2013.

[27] K. J. Njunwa, "Studies on the productivity of 'anopheles' breeding sites in relation to adult mosquito density," *London School of Hygiene and Tropical Medicine*, 1993.

[28] W. Mamai, L. N. Lobb, N. S. Bimbilé Somda, H. Maiga, H. Yamada, R. S. Lees, J. Bouyer, and J. R. L. Gilles, "Optimization of mass-rearing methods for anopheles arabiensis larval stages: Effects of rearing water temperature and larval density on mosquito life-history traits," *Journal of Economic Entomology*, vol. 111, pp. 2383–2390, 07 2018.

[29] C. Christiansen-Jucht, P. E. Parham, A. Saddler, J. C. Koella, and M.-G. Basáñez, "Temperature during larval development and adult maintenance influences the survival of anopheles gambiae s.s.," *Parasit Vectors*, vol. 7, p. 489, Nov 2014.

[30] Y. A. Afrane, G. Zhou, B. W. Lawson, A. K. Githeko, and G. Yan, "Effects of microclimatic changes caused by deforestation on the survivorship and reproductive fitness of anopheles gambiae in western kenya highlands.," *Am J Trop Med Hyg*, vol. 74, pp. 772–778, May 2006.

[31] I. Olayemi and A. Ande., "Survivorship of anopheles gambiae in relation to malaria transmission in ilorin, nigeria," *Online J Health Allied Scs*, vol. 7, no. 3, p. 1, 2008.

[32] World Health Organization, "Global malaria programme: Vector control." `https://www.who.int/teams/global-malaria-programme/prevention/vector-control`.

[33] C. Shiff, "Integrated approach to malaria control," *Clinical Microbiology Reviews*, vol. 15, no. 2, pp. 278–293, 2002.

[34] J. Hemingway, R. Shretta, T. N. C. Wells, D. Bell, A. A. Djimdé, N. Achee, and G. Qi, "Tools and strategies for malaria control and elimination: What do we need to achieve a grand convergence in malaria?," *PLOS Biology*, vol. 14, pp. 1–14, 03 2016.

[35] J. Li, H. J. Docile, D. Fisher, K. Pronyuk, and L. Zhao, "Current status of malaria control and elimination in africa: Epidemiology, diagnosis, treatment, progress and challenges," *Journal of Epidemiology and Global Health*, vol. 14, no. 3, pp. 561–579, 2024.

[36] "Malaria prevention: an overview of the tools." Medicines for Malaria Venture.

[37] K. Toé, C. M. Jones, S. N'Fale, H. M. Ismail, R. K. Dabiré, and H. Ranson, "Increased pyrethroid resistance in malaria vectors and decreased bed net effectiveness, burkina faso.," *Emerg Infect Dis*, vol. 20, pp. 1691–1696, Oct 2014.

[38] M. N. Bayoh and S. W. Lindsay, "Effect of temperature on the development of aquatic stages of anopheles gambiae sensu stricto (diptera: Culicide)," *Bulletin of Entomological Research*, vol. 93, pp. 375–381, 2003.

[39] M. N. Bayoh and S. W. Lindsay, "Temperature-related duration of aquatic stages of the afrotropical malaria vector mosquito anopheles gambiae in the laboratory," *Medical and Veterinary Entomology*, vol. 18, pp. 174–179, 2004.

[40] C. P. McCormack, A. C. Ghani, and N. M. Ferguson, "Fine-scale modelling finds that breeding site fragmentation can reduce mosquito population persistence.," *Commun Biol*, vol. 2, p. 273, 2019.

[41] J.-M. O. Depinay, C. M. Mbogo, G. Killeen, B. Knols, J. Beier, J. Carlson, J. Dushoff, P. Billingsley, H. Mwambi, J. Githure, A. M. Toure, and F. Ellis McKenzie, "A simulation model of african anopheles ecology and population dynamics for the analysis of malaria transmission," *Malaria Journal*, vol. 3, no. 1, p. 29, 2004.

[42] K. P. Paaijmans, M. O. Wandago, A. K. Githeko, and W. Takken, "Unexpected high losses of anopheles gambiae larvae due to rainfall.," *PLoS One*, vol. 2, p. e1146, Nov 2007.

[43] C. Koenraadt, A. Githeko, and W. Takken, "The effects of rainfall and evapotranspiration on the temporal dynamics of anopheles gambiae s.s. and anopheles arabiensis in a kenyan village," *Acta Tropica*, vol. 90, no. 2, pp. 141–153, 2004.

[44] G. Gilioli and L. Mariani, "Sensitivity of anopheles gambiae population dynamics to meteo-hydrological variability: a mechanistic approach," *Malaria Journal*, vol. 10, no. 1, p. 294, 2011.

[45] T. Lehmann, A. Dao, A. S. Yaro, A. Adamou, Y. Kassogue, M. Diallo, T. Sékou, and C. Coscaron-Arias, "Aestivation of the african malaria mosquito, anopheles gambiae in the sahel.," *Am J Trop Med Hyg*, vol. 83, pp. 601–606, Sep 2010.

[46] M. T. White, J. T. Griffin, T. S. Churcher, N. M. Ferguson, M.-G. Basáñez, and A. C. Ghani, "Modelling the impact of vector control interventions on anopheles gambiae population dynamics," *Parasites & Vectors*, vol. 4, no. 1, p. 153, 2011.

[47] G. J. Abiodun, R. Maharaj, P. Witbooi, and K. O. Okosun, "Modelling the influence of temperature and rainfall on the population dynamics of anopheles arabiensis," *Malaria Journal*, vol. 15, no. 1, p. 364, 2016.

[48] E. A. Mordecai, K. P. Paaijmans, L. R. Johnson, C. Balzer, T. Ben-Horin, E. de Moor, A. McNally, S. Pawar, S. J. Ryan, T. C. Smith, and K. D. Lafferty, "Optimal temperature for malaria transmission is dramatically lower than previously predicted.," *Ecol Lett*, vol. 16, pp. 22–30, Jan 2013.

[49] P. E. Parham and E. Michael, "Modeling the effects of weather and climate change on malaria transmission," *Environmental Health Perspectives*, vol. 118, no. 5, pp. 620–626, 2010.

[50] A. M. Lutambi, B. Emidi, F. G. Mbuya, M. Ryoba, T. D. Sagamiko, A. K. Hugo, and I. S. Mbalawata, "Modelling the impact of climatic and environmental variables on malaria incidence in tanzania: Implications for achieving the who's 2030 targets," *PLOS Global Public Health*, vol. 5, pp. 1–18, 08 2025.

[51] S. S. Kiware, N. Chitnis, A. Tatarsky, S. Wu, H. M. S. Castellanos, R. Gosling, D. Smith, and J. M. Marshall, "Attacking the mosquito on multiple fronts: Insights from the vector control optimization model (vcom) for malaria elimination," *PLOS ONE*, vol. 12, pp. 1–19, 12 2017.

[52] L. M. Beck-Johnson, W. A. Nelson, K. P. Paaijmans, A. F. Read, M. B. Thomas, and O. N. Bjørnstad, "The effect of temperature on anopheles mosquito population dynamics and the potential for malaria transmission.," *PLoS One*, vol. 8, no. 11, p. e79276, 2013.

[53] L. M. Beck-Johnson, W. A. Nelson, K. P. Paaijmans, A. F. Read, M. B. Thomas, and O. N. Bjørnstad, "The importance of temperature fluctuations in understanding mosquito population dynamics and malaria risk.," *R Soc Open Sci*, vol. 4, p. 160969, Mar 2017.

[54] E. O. Asare, A. M. Tompkins, L. K. Amekudzi, and V. Ermert, "A breeding site model for regional, dynamical malaria simulations evaluated using in situ temporary ponds observations," *Geospatial health*, vol. 11, 2016.

[55] M. Mann Manyombe, B. Tsanou, J. Mbang, and S. Bowong, "A metapopulation model for the population dynamics of anopheles mosquito," *Applied Mathematics and Computation*, vol. 307, pp. 71–91, 2017.

[56] H. S. Ngowo, F. O. Okumu, E. E. Hape, I. H. Mshani, H. M. Ferguson, and J. Matthiopoulos, "Using bayesian state-space models to understand the population dynamics of the dominant malaria vector, anopheles funestus in rural tanzania," *Malaria Journal*, vol. 21, no. 1, p. 161, 2022.

[57] D. A. Ewing, B. V. Purse, C. A. Cobbold, S. M. Schäfer, and S. M. White, "Uncovering mechanisms behind mosquito seasonality by integrating mathematical models and daily empirical population data: Culex pipiens in the uk," *Parasites & Vectors*, vol. 12, no. 1, p. 74, 2019.

[58] R. Nisbet and W. Gurney, "The systematic formulation of population models for insects with dynamically varying instar duration," *Theoretical Population Biology*, vol. 23, pp. 114–135, 1983.

[59] D. P. Brass, C. A. Cobbold, B. V. Purse, D. A. Ewing, A. Callaghan, and S. M. White, "Role of vector phenotypic plasticity in disease transmission as illustrated by the spread of dengue virus by aedes albopictus," *Nature Communications*, vol. 15, no. 1, p. 7823, 2024.

[60] F. Ishtiaq, S. Swain, and S. S. Kumar, "Anopheles stephensi (asian malaria mosquito)," *Trends in Parasitology*, vol. 37, no. 6, pp. 571–572, 2021.

[61] K. Birungi, D. P. Mabuka, V. Balyesima, F. Tripet, and J. K. Kayondo, "Attributes of anopheles gambiae swarms in south central uganda.," *Parasit Vectors*, vol. 17, p. 149, Mar 2024.

[62] L. Molineaux and G. Gramiccia, "The garki project: research on the epidemiology and control of malaria in the sudan savanna of west africa," *World Health Organization*, 1980.

[63] D. Padfield and H. O'Sullivan, "rtpc: Fitting and analysing thermal performance curves." https://github.com/padpadpadpad/rTPC, 2023.

[64] U. Fillinger, H. Sombroek, S. Majambere, E. van Loon, W. Takken, and S. W. Lindsay, "Identifying the most productive breeding sites for malaria mosquitoes in the gambia.," *Malar J*, vol. 8, p. 62, Apr 2009.

[65] C. Rackauckas and Q. Nie, "Differentialequations.jl–a performant and feature-rich ecosystem for solving differential equations in julia," *Journal of Open Research Software*, vol. 5, no. 1, p. 15, 2017.

[66] K. Soetaert, T. Petzoldt, and R. W. Setzer, "Solving differential equations in r: Package desolve," *Journal of Statistical Software*, vol. 33, no. 9, pp. 1–25, 2010.

[67] C. Christiansen-Jucht, K. Erguler, C. Y. Shek, M.-G. Basáñez, and P. E. Parham, "Modelling anopheles gambiae s.s. population dynamics with temperature- and age-dependent survival," *International Journal of Environmental Research and Public Health*, vol. 12, no. 6, pp. 5975–6005, 2015.

[68] J. Baafi and A. Hurford, "Modeling the impact of seasonality on mosquito population dynamics: Insights for vector control strategies," *Bulletin of Mathematical Biology*, vol. 87, no. 2, p. 33, 2025.

[69] F. Simard, D. Ayala, G. C. Kamdem, M. Pombi, J. Etouna, K. Ose, J.-M. Fotsing, D. Fontenille, N. J. Besansky, and C. Costantini, "Ecological niche partitioning between anopheles gambiae molecular forms in cameroon: the ecological side of speciation," *BMC Ecology*, vol. 9, no. 1, p. 17, 2009.